ACKNOWLEDGMENTS

I wish to express my gratitude and appreciation to Dr. Erol Emre for his support and encouragement throughout the course of my research. I would also like to thank my thesis committee members Dr. Kwong S. Chao and Dr. Donald Gustafson for their invaluable guidance. The faculty and staff of the Electrical Engineering Department facilitated my research greatly and I extend my most sincere appreciation for their help.

Chintanie Wettasinghe, my colleague, assisted me immensely during the research and I take this opportunity to recognize her contribution. Tina Vigstol, by being her efficient self, eased the way towards the completion of my research. I finally would like to acknowledge the very significant contributions of my family and friends who have believed in me and made this dream a reality.

TABLE OF CONTENTS

ABSTRACT

This thesis is the presentation of an investigation into a classical bandlimited function extrapolation technique, namely the Papoulis-Gerchberg algorithm. This algorithm can be used in the field of RADAR signal processing to estimate the Time-Varying Target Density function of a moving target at different points in space in accordance with methods developed by Dr. Emre. The estimation of the Target Density function yields a scaled estimate of the effective cross-section of the target at that point. With all spatial points combined we would receive a picture of the target space at each time point. This would form, in effect, a real time image of the target space. The study consists of exploring the capabilities of the Papoulis-Gerchberg algorithm, thereby evaluating its possible use in the algorithm for estimating the Time-Varying Target Density function. The study also explores the effectiveness of the Papoulis-Gerchberg algorithm when applied to a bandlimited Target Density function. The two algorithms were simulated using MATLAB and the results were generated as comparisons between MATLAB charts.

LIST OF FIGURES

CHAPTER I

INTRODUCTION

This thesis consists of an exploration of the capabilities of the Papoulis-Gerchberg algorithm. This algorithm is used for bandlimited extrapolation. An application of the algorithm in Dr. Emre's algorithm for the estimation of Time-Varying Target Density functions is also shown.

1.1 The Fourier Transform

The Fourier transform $F(\omega)$, of a function $f(t)$ can be derived as follows.

$$F(\omega) = \int_{-\infty}^{\infty} f(t)e^{-j\omega t}dt .$$

For a signal bandlimited to $\pm\sigma$, the Inverse Fourier transform is

$$f(t) = \frac{1}{2\pi}\int_{-\sigma}^{\sigma} F(\omega)e^{j\omega t}d\omega .$$

The above two transforms play a vital role in the extrapolation techniques investigated.

1.2 The Problem of Extrapolation

In nature, there is no practical way to observe a signal for infinite time. Only a finite segment of any signal can be recorded and, based upon this known segment, the

rest of the signal up to the time desired must be predicted using an estimation method. This is one of the major problems in Fourier Analysis and Spectral Estimation. A solution to this problem would be to approximate the frequency spectrum of the time signal segment and from this result attempt to reconstruct the rest of the time signal. Numerous methods to accomplish this have been proposed. These methods include the Windowing technique (or Short Time Fourier Transform), the use of modern ARMA models and the use of Prolate Spheroidal functions, to name but a few. However, one of the most well-documented classical methods for signal extrapolation has been the Papoulis-Gerchberg algorithm. During the course of the preliminary research that led to this thesis, the Papoulis-Gerchberg algorithm was found to be the most pertinent and effective for the purposes of bandlimited extrapolation.

1.3 The Windowing technique

If only a segment up to time T of a function f(t) is known, then its Fourier transform can be estimated by transforming the product of the segment with a window, w(t), which is suitably chosen to reduce errors, i.e.,

$$F(\omega) = \int_{-T}^{T} w(t) f(t) e^{-j\omega t} dt.$$

w(t) is any standard window as shown in Figure 1.1.

$$w(t) = 1, |t| \leq T$$
$$w(t) = 0, |t| > T$$

This gives a rough estimate of the frequency spectrum. The obvious drawback in this is that the portion of the windowed time signal after time T will still be zero after the inverse transform. Therefore some a priori assumptions have to be made about the form of the function in order to extrapolate the function.

1.4 Overview of the Papoulis-Gerchberg algorithm

The Papoulis-Gerchberg algorithm is a spectral estimation method for computing the spectra of bandlimited functions. It is a successive iteration procedure involving only the Fourier transform and its inverse transform. By estimating the spectra of bandlimited functions, it is possible to extend the known time series past the time of observation. The Papoulis-Gerchberg algorithm has been found (1) to be more effective in accurately predicting the time function than any estimation method involving a priori assumptions, like the Windowing technique. A comprehensive study of this algorithm is presented in the next chapter.

1.5 The concept of a Target Density function

The Target Density function is the indication of the RADAR cross section of each target at each point in space. The points in space can be expressed as range and angle pairs. The Target Density functions can be processed to yield an image of the target area. This function is also called the Target Reflectivity function. The Target Density function is a function of time at each point in space.

1.6 Formulation of the thesis problem

The aim of this thesis is to investigate the accuracy and speed of the Papoulis-Gerchberg algorithm. It also aims to demonstrate its possible use in the field of RADAR for the estimation of the signal representing the Time-Varying Target Density function of a target in space. The problem we are faced with regarding bandlimited extrapolation is the estimation of the time series samples, up to (ideally) an infinite number of samples given a finite number of samples of the signal and the fact that it is bandlimited. The scope of this investigation can be summarized as follows.

a. To verify that the Papoulis-Gerchberg algorithm does indeed perform extrapolation of a bandlimited time series.

b. To investigate the effect of the number of iterations of the algorithm on the accuracy of the estimate.

c. To investigate the effects of different sampling rates and the number of samples available on the accuracy of the estimate.

d. To demonstrate the possibilities of the application of the Papoulis-Gerchberg algorithm. This is to be done via a demonstration of Dr. Emre's algorithm to estimate the Time-Varying Target Density function of a target in space. The signal being worked on is actually a set of 10 signals received by an array of sensors over finite time from all points in the target space.

e. To verify Dr. Emre's algorithm by estimating the time series that represents the Time-Varying Target Density function.

f. To familiarize the reader with the advantages of the Target Density function approach over conventional RADAR techniques.

Practical constraints however limit our extrapolation of the samples to 2000 estimated samples given only 20 samples. It is proposed to define a bandlimited function in the frequency domain and to truncate its samples in the time domain to 20. This segment is to be subjected to the Papoulis-Gerchberg algorithm and its performance analyzed by comparison with the original time series. A convergence plot is to be generated. This is to show the effect of the number of iterations on the algorithm. The aim of this also extends to a demonstration of the practical use of the Papoulis-Gerchberg algorithm in Dr. Emre's algorithm for estimation of the time series representing the Time-Varying Target Density function of a target in space. A comparison between a synthesized time series and its estimate is presented visually.

1.7 Overview of the thesis

This thesis is divided into chapters. Their content has been summarized below. Chapter II covers the actual Papoulis-Gerchberg algorithm along with a treatment of the effects of noise on the algorithm. Chapter III seeks to familiarize the reader with the concept of a Target Density Function and its advantages over conventional RADAR techniques. Chapter IV presents Dr. Emre's algorithm for the estimation of a

time-varying Target Density function.Chapter V covers the aspects of implementation of Dr. Emre's algorithm. Chapter VI presents the results of the thesis and draws conclusions from them. These chapters are then followed by the actual results and the source code of the program that implemented them.

CHAPTER II

THE PAPOULIS-GERCHBERG ALGORITHM

The Papoulis-Gerchberg algorithm is a method for extrapolating f(t) and its transform $F(\omega)$ from a given segment of the signal f(t). This method involves the discrete Fourier series and a Fast Fourier transform (FFT) along with its inverse transform. It is an iteration method for computing the Fourier transform of a band-limited function.

2.1 Working of the algorithm

We wish to determine the Fourier transform of a function f(t) bandlimited in frequency in terms of the finite segment g(t) of f(t),

$$g(t) = f(t)p_T(t),$$

where

$$p_T(t) = 1, |t| \leq T$$
$$p_T(t) = 0, |t| \rangle T.$$

The Papoulis-Gerchberg algorithm starts the iteration by taking the Fourier transform of the given segment $g(t) = g_0(t)$,

$$G(w) = G_0(w) = \int_{-T}^{T} g_0(t)e^{-jwt}dt.$$

The nth iteration step of the algorithm proceeds by forming the function

$$F_n(w) = G_{n-1}(w)p_s(w) \quad ,$$

where

$$p_s(w) = 1, |w| \leq s$$
$$p_s(w) = 0, |w| > s.$$

Therefore, $F_n(\omega)$ is obtained by truncating $G_{n-1}(\omega)$. Then, the inverse Fourier transform of $F_n(\omega)$ is as follows:

$$f_n(t) = \int_{-s}^{s} F_n(w)e^{jwt}dw \, .$$

The next form of the function is,

$$g_n(t) = f_n(t) + [f(t) - f_n(t)]p_T(t) = \begin{matrix} g(t), |t| \leq T \\ f_n(t), |t| > T \end{matrix}$$

obtained by replacing the segment of $f_n(t)$ in the interval (-T,T) by the known segment g(t) of f(t). This iteration is equivalent to the analog model in Figure 2.1 with the gate switching states at time T. The nth step ends by computing the transform,

$$G_n(w) = \int_{-\infty}^{\infty} g_n(t)e^{-jwt}dt \, .$$

The various steps associated with the algorithm may be seen in Figure 2.2.
Finally, it can be shown that (1), as in Figure 2.3,

$$f_n(t) \rightarrow f(t)$$
$$F_n(w) \rightarrow F(w) \qquad \text{as} \quad n \rightarrow \infty.$$

2.2 Implementation of the algorithm

Suppose the spectrum $F(\omega)$ of an arbitrary band-limited function is given at 2000 data points. Then we find $f(t)$ by taking the inverse Fourier transform (IFT) of $F(\omega)$. By considering only a segment of this time function f(t) to be available, i.e., g(t), we apply the algorithm to g(t) to obtain approximations for f(t) and $F(\omega)$ after a number of iterations, here assumed arbitrarily to be 100. Comparisons between original time function f(t) and approximated time function $f_n(t)$, and spectrum $F(\omega)$ and approximated spectrum $F_n(\omega)$ were performed. The algorithm was applied arbitrary spectra $F(\omega)$, listed in the results, which all had the common characteristic of being bandlimited. The number of discrete points where the functions were evaluated was fixed to be 2000, so as to allow the time function to asymptotically approach zero in all cases. T was chosen to be 20 and σ was chosen to be 200 for simplicity. For truncating the frequency spectrum after σ, a fifth-order lowpass filter, defined via the Yule-Walker equations was used. This was done to simulate analog filtering as closely as possile. The time function was scaled to be at the Nyquist Sampling rate. Both the imaginary and real parts of the time functions were presented for comparison. Also, the RMS error between the extrapolated and the actual functions was observed and the convergence of the extrapolated function to the actual function was plotted as a function of the number of iterations. The preceding analysis was carried out on time functions scaled to be at the Nyquist Sampling rate.Then, the

same analysis was carried out on the same functions sampled at twice the previous rate of sampling. Thus, the number of points initially available was increased as was the accuracy of the sampled time waveform. The convergence curve is shown for this case too. The time functions chosen were the time domain representations of the bandlimited functions formed in the frequency domain.

All the above simulations of the algorithm were processed on MATLAB v 4.2, running on a Pentium 60 Mhz processor. Signal Processing and Symbolic Math toolboxes provided most of the functions that were implemented.

2.3 The effects of noise on the algorithm

The algorithm is already heavily corrupted by noise in the discretization process of the analog signal, the generated signals having being sampled at the Nyquist Sampling Rate or slightly higher. To this, ambient white noise is also added in the practical case due to the noise contributed by the atmosphere and other external factors. However, in utilizing the Papoulis-Gerchberg algorithm in the estimation of the Target Density function, the discretization noise and integral approximation errors in the original function are so great that this noise would be insignificant. Regardless of that, the effects of white noise on the algorithm merit inclusion. The Signal-to-Noise ratios dealt with lay in the range of 10 to 20 dB.

Generally speaking, the algorithm is affected by the following errors.

2.3.1 Truncation of the iteration

It has been proved by Papoulis (1) that if

$$f(t) = \sum_{k=0}^{\infty} a_k \phi_k(t),$$

where $\phi_k(t)$ s are called prolate spheroidal functions and a_ks are their coefficients, then

$$F_n(\omega) - F(\omega) = B\, p_\sigma(\omega) \sum_{k=0}^{\infty} a_k \sqrt{\lambda_k}\,(1-\lambda_k)^n \phi_k(b\omega),$$

where

$$B = \sqrt{\frac{2\pi T}{\sigma}}, \qquad b = \frac{T}{\sigma}.$$

λ_k s are the eigenvalues of the prolate spheroidal functions.

T is the number of time points available befire extrapolation.

So as $n \to \infty$, $F_n(\omega) \to F(\omega)$, since λ_k lies between 0 and 1. However it is not possible to compute the transform after an infinite number of iterations. So, after n iterations, the mean-square error is given by

$$E_n = \frac{1}{2\pi} \int_{-\sigma}^{\sigma} |F(\omega) - F_n(\omega)|^2 \, d\omega$$

$$= \sum_{k=0}^{\infty} a_k^2 (1-\lambda_k)^{2n}.$$

In the Figure 2.4, we see that the eigenvalues increase with the product σT, resulting in a decrease in the error.

Thus we can say that the higher the bandwidth-time product, the fewer the number of iterations needed to achieve the same accuracy. The coefficients a_k s also contribute as n increases. They also become particularly important when σ exceeds the bandwidth of the signal. Thus we can conclude that for optimal performance σ must be in the neighborhood of the bandwidth of the signal.

2.3.2 Aliasing error

Although we assumed a bandlimited function is the only kind we would be operating upon, there will still be high-frequency components outside the assumed frequency range in practical cases. If the energy of these high frequency components is small, they can be neglected. If not, aliasing occurs and the noise contributed by these high frequency components is approximately given by

$$E_{nh} = n^2 E_h.$$

where E_h is the energy contributed by the high frequency components.

2.3.3 White noise

If white noise n(t) that has a spectral density S, is added to the original time segment, then the mean square error contributed by it at the n^{th} iteration is given by

$$R_n \leq 2STn^2.$$

2.3.4 Roundoff error

In the process of transforming any analog signal into a digital form, we lose some accuracy. However, if these roundoff errors are independent and have a standard deviation q, then they can be compared to white noise with $S=q^2\delta$, δ being the sampling interval and the resulting error can be easily deduced.

2.3.5 Other errors

There are others errors which need to be taken into consideration too. The error due to the lack of a sharp cutoff has been minimized by using a fifth-order filter. The estimation of the Fourier transform via Fourier series also introduces an unavoidable error.

This chapter served as a comprehensive treatment of the Papoulis-Gerchberg algorithm. The next chapter introduces the Target Density function, in whose estimation the Papoulis-Gerchberg algorithm is to be used.

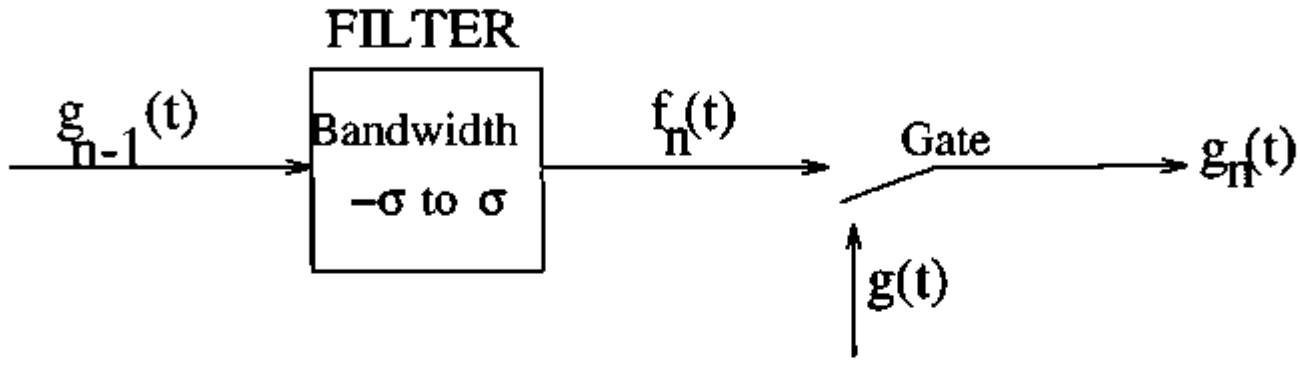

Figure 2.1 Analog Simulation of an iteration of the Papoulis-Gerchberg algorithm

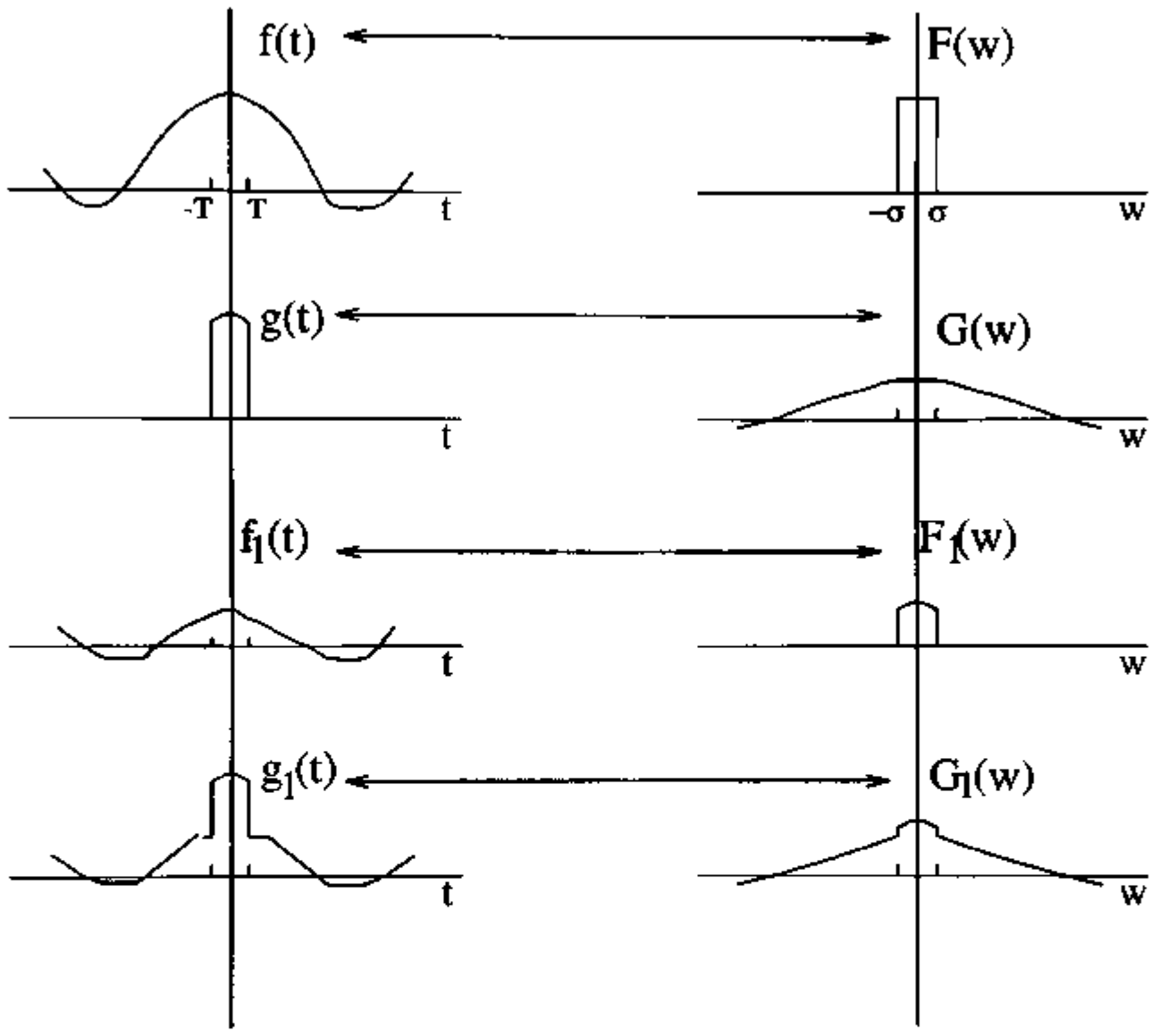

Figure 2.2 Signals of the 1st iteration of the Papoulis-Gerchberg algorithm

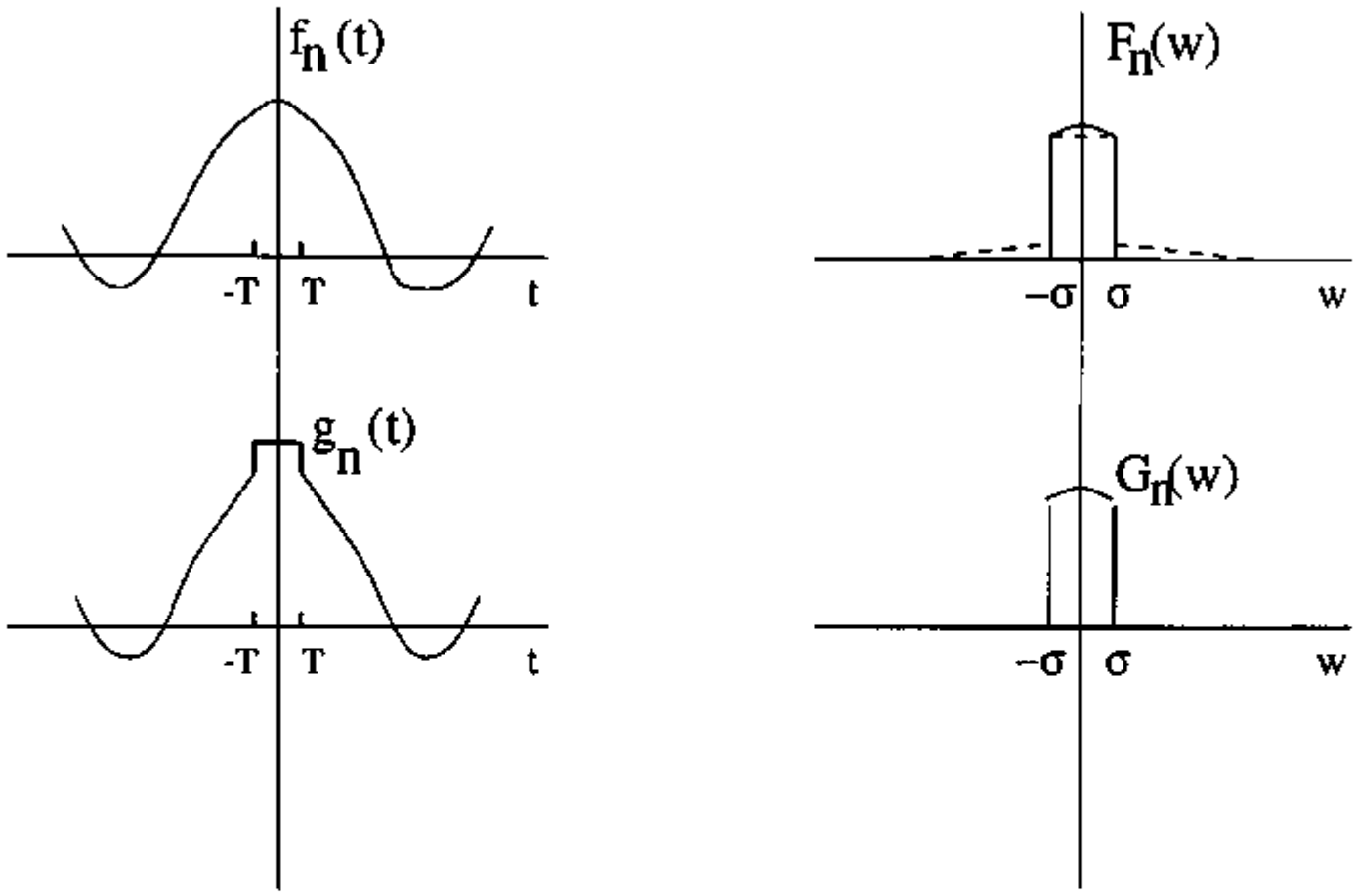

Figure 2.3 Signals of the nth iteration of the Papoulis-Gerchberg algorithm

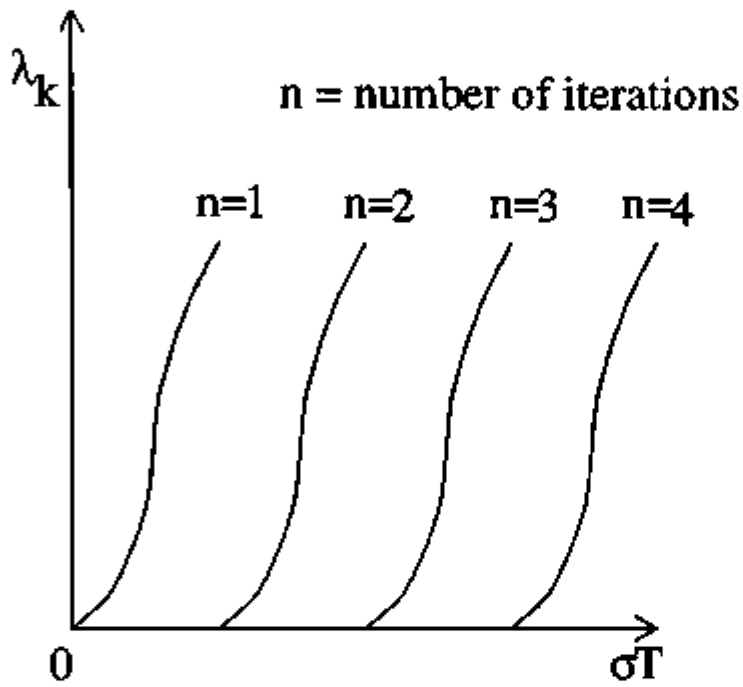

Figure 2.4 Eigenvalues of the Prolate Spheroidal Functions versus Time-Bandwidth Product

CHAPTER III

THE TARGET DENSITY FUNCTION APPROACH TO RADAR

3.1 The drawbacks of current RADAR systems

The techniques presently adopted in RADAR systems are beset with some limitations which contribute to make the system less effective. Some of the major problems are outlined below.

3.1.1 Clutter and Glint

Clutter is defined to be the signal returned from extraneous sources due to the RADAR beam intercepting them. Some examples of such sources are large buildings, towers and most important, the sea and land. In the latter case the signal returned is termed ground clutter and is indicated by c_h, homogeneous clutter in the Figure 3.1. c_d represents discrete clutter due to the smaller targets. The clutter considerably degrades RADAR performance particularly in application to small target detection. In conventional pulsed RADAR techniques, clutter creates a difficulty in discriminating the source of clutter from actual moving targets, especialy for low PRF RADAR systems. In Doppler RADAR, for a roaming RADAR system, the clutter comes into prominence. In current RADAR systems, the system scans the target area at each point by angular beamforming as in Figure 3.2, but due to finite aperture, sidelobes, as shown in Figure 3.2 invariably result and these contribute to clutter.

Glint is the error caused by interference between signals returned from different parts of the same target. For extended targets this error is quite pronounced. The presence of the aforementioned sidelobes further compounds the error.

3.1.2 Data Association

A fundamental assumption of conventional pulsed RADAR is the concept of a stationary target. Here, the target is assumed to be stationary throughout the time required for the processing of the returned signal. This leads to a significant discretization in position estimation of the target because the target may not actually be stationary. The extent of discretization would depend on the velocity of the target relative to the sensor. So we do not have a determined trajectory for the target and would have to resort to data association techniques to approximate the trajectory. In multi-target tracking the data association would have to take into account, the following problems.

a. Spurious signals causing false alarms.

b. Clutter.

c. Interfering targets and decoys.

All of the above would lead to an error in the actual target trajectory estimation. Also Doppler RADAR would give us information only about the target's radial velocity (12).

3.2 Advantages of the Target Density function approach

The Target Density function approach accounts for the actual shape of the beamform and compensates for the sidelobes and the distributed main lobe. So we can utilize energy efficient beamforms even with very large sidelobes and thus we can minimize clutter and glint from the signal.

This concept also provides for the accomodation of motion during the processing period. We can obtain as many measurements as we need for each processing period, thus almost eliminating the need for data association and the errors inherent with it.

Using the Target Density function approach, we can with proper pre-calibration estimate all components of the velocity of the target.

3.3 The types of Target Density functions

3.3.1 Time invariant Target Density function

This type of Target Density function is found wherever there are large stationary objects. As such, it can be seen in satellite imaging applications, depth charting etc., where any relative motion between the target and sensor is small enough to be negligible.

3.3.2 Time-Varying Target Density function

With most RADAR targets, especially in defense applications the targets are moving at a very rapid velocity relative to the sensor. In such cases, the reflectivity of each point in space varies within a relatively short time. This change gives rise to the concept of the Time-Varying Target Density function. By estimating it at each point in time we can obtain what amounts to a moving picture of the target area. We can also thus accomplish multi-target tracking.

3.4 Conditions for the existence of a Target Density function

It has been proven (1) that a Target Density function is indeed an accurate indication of the target cross section and also that the Target Density function physically exists and is practically measurable. However, the following conditions constrain its existence and usefulness for estimating the RADAR cross section of a target.

a. The transmitted signal is continuous.

b. The signal is monochromatic or very narrow band.

If the signal described above is modulated by a pulse train, the Target Density function still exists. If an additional requirement that the Target Density function be bandlimited in nature were to be introduced, the extra condition for its existence would be that the variation in motion of the target be limited. This is a practical assumption since aircraft cannot produce an infinite variety of motion.

3.5 Physical interpretation of the Target Density function

The Target Density function is meaningless unless a physical parameter can be inferred from its characteristics. In this case the parameter would be the RADAR cross section. If a signal $W(t)$ is transmitted, then the returned signal from a minute portion of the target space is given by S_r, where

$$S_r = h(t, R, \beta)W(t)\delta R\,\delta\beta \ .$$

where

δR is a small increment in radial distance from phase center.

$\delta\beta$ is a very small angle subtended at the phase center.

$h(t, R, \beta)$ is the reflectivity of the small area.

The Target Density function is just the reflectivity of each point in space. So, if a target is present it is illuminated by the transmitted signal and reflects part of the signal back to the sensor. So the target itself acts as an emitter. This implies that if no target were to be present, the signal returned would be zero. We can see logically that the strength of the returned signal is proportional to the target's cross section at a constant range. Some deductions can be made from this.

a. The strength of the Target Density function indicates the cross section of the target at that point in space and moment in time.

b. The edges of the target would appear as delta functions in the Target Density function due to the sudden transition from the presence of the target to an absence.

c. With proper mapping the Target Density function can be transformed into intensity values thus yielding the desired motion picture of the sky. The Target Density function also has the property of being positive always, since being negative implies that the target draws out more than the transmittted signal power from the transmitter and does not reflect any amount of signal. Since the perfectly absorbing 'black box' is physically unrealizable, the property mentioned would be valid.

This chapter has outlined the drawbacks of current RADAR systems and introduced the concept of a Target Density function as a means of minimizing them. The next chapter describes Dr. Emre's algorithm for the estimation of a time-varying Target Density function.

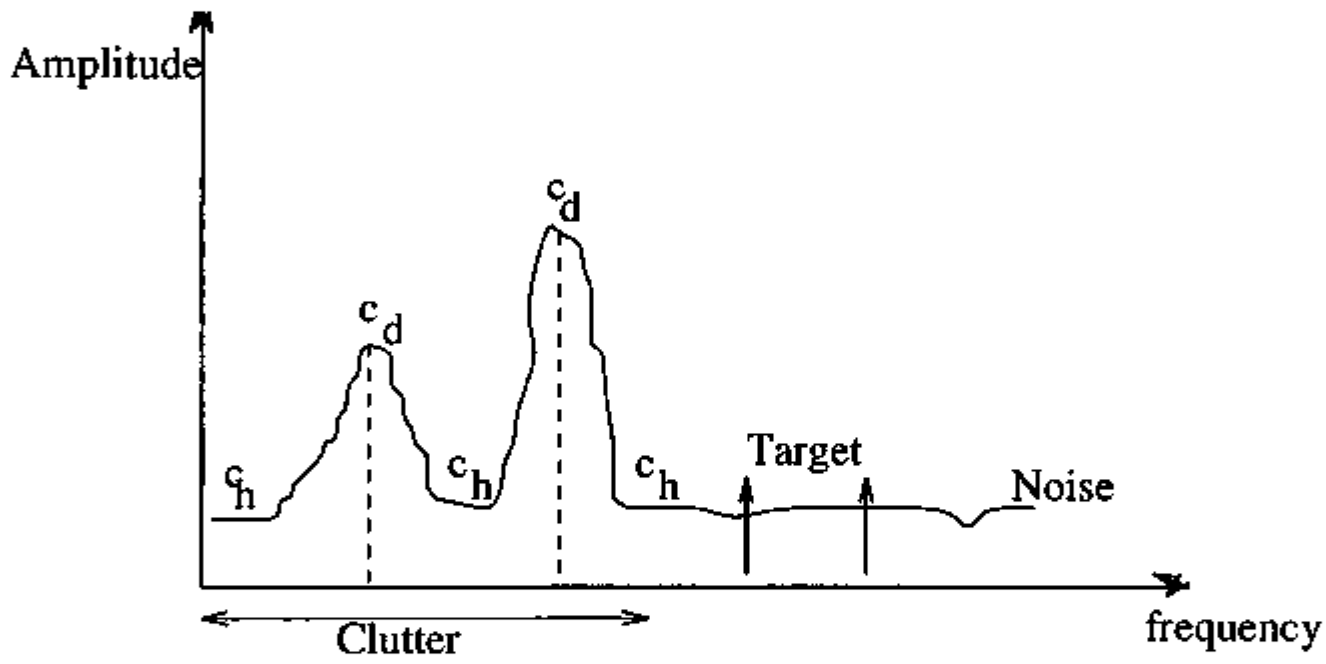

Figure 3.1 Spectrum of the signal returned to a sensor from the target space

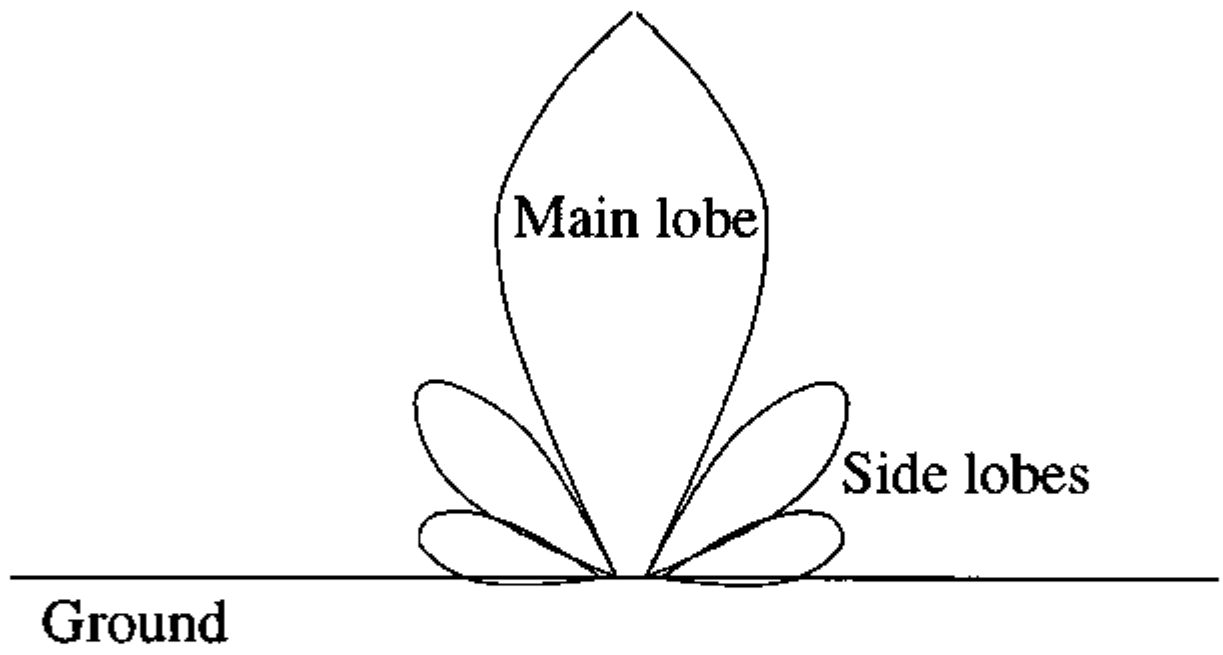

Figure 3.2 Beam Pattern of a conventional transmitting antenna

CHAPTER IV

A TECHNIQUE FOR ESTIMATION OF THE TIME-VARYING TARGET DENSITY FUNCTION

In this chapter, a technique for the estimation of a bandlimited time-varying Target Density function is described. What follows is an outline of the algorithm and an explanation of its discrete steps. These steps are at the signal processing level. The signal has already been acquired by an array of sensors.

4.1 An overview of target space and the sensor array

For the sake of simplicity we view 3-dimensional target space in 2-dimensions. The rest of this thesis deals with the target space as if it were indeed two-dimensional. The target space is hence represented in terms of β, the cosine of the angle subtended by the point in space with the ground and R, the range of the target as measured from the indicated phase center. The parameter β varies from -1 to 1 as θ varies from $-\pi$ to π and R varies from 0 to R_1, where R_1 is the maximum range from which backscattering occurs. The method of calculating this distance is given in equation 4.4. The sensor array is a set of individual sensors spaced a quarter of transmitted carrier wavelength ($\lambda/4$) apart from each of its neighbors.

4.2 The algorithm for estimating the Target Density function

We initially assume that we have transmitted a signal of the form

$$W(\beta,t) = \sum_{k=-M}^{M} q_k(\beta)e^{jk\omega_0 t}. \qquad ...4.1$$

An example of this kind of signal is given in equation 4.2 where a pulse train modulates the carrier signal shaped into a conventional beamform. The previous chapter talked about the need for a monochromatic signal (or its product with a pulse train) to be transmitted in order that a Target Density function exist. We can see that the signal in equation 4.2 satisfies this condition.

$$W(\beta,t) = e^{j\omega_c t}\, q(\beta)\, p(t), \qquad ...4.2$$

$e^{j\omega_c t}$: *carrier*,

$q(\beta)$: *a conventional beamform*,

$p(t)$: *a train of pulses of PRF* ω_0.

k from equation 4.1 depends on the carrier frequency and the PRF. For a carrier frequency of 100 Mhz and a PRF of 100 Khz, k would range from (1000-M) to (1000+M) assuming we take only 2M+1 samples of the time function contributed by the target.

For simplicity, take

$$\omega_c = 0.$$

$$\omega_o = 2\pi / T,$$

$$1/T = PRF\ (pulse\ \ repetition\ \ frequency).$$

It is however to be noted that in the practical case, the frequency spectrum would be shifted by the carrier frequency. Thus, for example,

$$W(\beta, t) = q(\beta)\, p(t),$$

(due to the hypothetical, notationally simplifying assumption that $\omega_c = 0$).

4.2.1 Target Density function

The below is the actual Target Density function that is to be estimated.

$$h(t, R, \beta) := \text{Reflectivity of the point } (R, \beta) \text{ at time t.}$$

i.e., if $e^{j\omega_c t}$ is transmitted, S_r would be the returned signal, where

$$S_r = h(t, R, \beta)\, e^{j\omega_c (t - \frac{R}{c})}\, x(\Delta R.\Delta\beta), \qquad ...4.3$$

is the return signal emanating from a very small area $(\Delta R.\Delta\beta)$ which includes the point (R, β). So we can assume each target in space to be acting as an infinite set of minute transmitters, each transmitting S_r which varies depending on the position. For a very small area $(\Delta R.\Delta\beta)$,

$$h(t, R, \beta)(\Delta R.\Delta\beta),$$

is very closely equal to the reflectivity of the point (β, R) at time t.

Define

$$H(\omega, R, \beta) := \int_{-\infty}^{\infty} h(t, R, \beta)\, e^{-j\omega t}\, dt, \text{ (Fourier transform).}$$

Define

$$\tilde{H}(\omega, R, \beta) := H(\omega, R, \beta)\, e^{-j\frac{\omega R}{c}}.$$

We will estimate the above quantity.

Note:

$$\tilde{H}(\omega, R, \beta) = F\{h(t - \frac{R}{c}, R, \beta)\}.$$

(F {h} := Fourier transform of h).

Also it is to be noted that $h(t, R, \beta) = 0$ for $R \notin [0, R_1]$, where R_1 is the maximum range from which there is backscattering.This R_1 can be calculated from the equation 4.3.

4.2.2 No range ambiguity condition

In RADAR systems, if the PRF remains constant, we have the possibility of an ambiguity occurring in the measurement of range of a target. This effect is due to the fact that the time it takes for a pulse to impact on a distant target and be reflected by it is greater than the time it takes for the next pulse to be transmitted. So, the RADAR receiver cannot decide which pulse caused the return signal leading to ambiguity in range. So the maximum range which can be determined without cause for doubt, R_1, is determined by the PRF and satifies equation 4.4, given below.

$$\frac{2\omega_o}{c} = \frac{2\pi}{R_1}. \qquad \text{...4.4}$$

c is the speed of light. This limitation on range is not very troublesome as the algorithm is designed for accurate tracking of targets, whose motion in most cases tends to become more unpredictable with decreasing range.

4.2.3 Implications of the "no range ambiguity condition"

Since

$$h(t, R, \beta) = 0 \quad for \quad R \notin [0, R_1],$$

we can say that for that particular range the contribution to the frequency spectrum would be negligible. i.e.,

$$H(\omega, R, \beta) = 0 \quad for \quad R \notin [0, R_1],$$

and

$$\tilde{H}(\omega, R, \beta) = 0 \quad for \quad R \notin [0, R_1].$$

Next consider the Fourier Transform of $\tilde{H}(\omega, R, \beta)$ with respect to R.

Call it

$$\overline{\tilde{H}}(\omega, w, \beta) := \int_{-\infty}^{\infty} \tilde{H}(\omega, R, \beta)\, e^{-jwR} dR$$

$$= \int_{0}^{R_1} \tilde{H}(\omega, R, \beta)\, e^{-jwR} dR.$$

Thus $\overline{\tilde{H}}(\omega, w, \beta)$ is a bandlimited function of w, for each fixed (ω, β), lending itself for the operation of bandlimited extrapolation. If we know its value for w in a

certain interval this will determine $\tilde{\tilde{H}}(\omega, w, \beta)$ for all w, within reason by extrapolating via the Papoulis-Gerchberg algorithm.

We will next estimate

$$\tilde{\tilde{H}}(\omega, k\frac{2\omega_o}{c}, \beta) \quad \text{for} \quad -M \le k \le M.$$

Then extrapolation will yield an estimate of $\tilde{\tilde{H}}(\omega, w, \beta)$ for all w.

Let

$$H_k(\omega, \beta) \;:=\; \tilde{\tilde{H}}(\omega, k\frac{2\omega_o}{c}, \beta).$$

The purpose of the algorithm now degenerates to the estimation of $H_k(\omega, \beta)$.

Considering the Fourier Series expansion of $\tilde{H}(\omega, R, \beta)$ over the interval $[0, R_1]$,

$$\tilde{H}(\omega, R, \beta) \;=\; \sum_{k=-M}^{M} \tilde{H}_k(\omega, \beta)\, e^{jkw_1 R},$$

where

$$w_1 \;=\; \frac{2\pi}{R_1}.$$

The similarity of the R term to time in conventional space and w to frequency is to be noted above. From the no ambiguity condition equation 4.3,

$$w_1 = \frac{2\omega_o}{c},$$

So,

$$\tilde{H}_k(\omega, \beta) \;=\; \frac{1}{R_1}\int_0^{R_1} \tilde{H}(\omega, R, \beta)\; e^{-jk\frac{2\omega_o}{c}R}\, dR$$

$$= \frac{1}{R_1} H_k(\omega, \beta),$$

where the quantity to be estimated is

$$H_k(\omega, \beta) = \overline{\tilde{H}}(\omega, k\frac{2\omega_o}{c}, \beta), \quad -M \le k \le M.$$

4.2.4 Assumption of the form of the Target Density function

h(t, R, β) is bandlimited, as a function of t for each fixed (R,β), i.e.,

$$H(\omega, R, \beta) = \tilde{H}(\omega, R, \beta) = 0 \quad for \quad |\omega| > \frac{\omega_o}{2}.$$

Now we proceed to estimate $H_k(\omega, \beta)$.

The total back scattered signal received by the sensor at the point x is

$$y(x,t) = \int_0^{R_1} \int_{-1}^{1} h(t - \frac{R}{c} - \frac{\beta x}{c}, R, \beta) W(\beta, t - \frac{2R}{c} - \frac{\beta x}{c}) d\beta \, dR,$$

h(t,R,β) can be written as

$$h(t, R, \beta) = \frac{1}{2\pi} \int_{-\omega_o/2}^{\omega_o/2} H(\omega, R, \beta) e^{j\omega t} d\omega.$$

by invoking the Inverse Fourier transform. Substitute this and W(β,t) in the integral,

to find

$$y(x,t) = \frac{1}{2\pi} \sum_{k=-M}^{M} e^{jk\omega_o t} \int_{-\omega_o/2}^{\omega_o/2} e^{j\omega t} \int_{-1}^{1} \int_{0}^{R_1} H(\omega, R, \beta) e^{-j\omega \frac{R}{c}} e^{-jk\frac{2\omega_o R}{c}} dR$$

$$\times q_k(\beta) e^{-j(\omega + k\omega_o)\frac{x\beta}{c}} d\beta \, d\omega. \quad ...4.5$$

The first (innermost) integral is

$H_k(\omega, \beta)$.

So,

$$y(x,t) = \frac{1}{2\pi} \sum_{k=-M}^{M} e^{jk\omega_o t} \int_{-\omega_o/2}^{\omega_o/2} e^{j\omega t} \int_{-1}^{1} q_k(\beta) H_k(\omega, \beta) e^{-j(\omega+k\omega_o)\frac{x\beta}{c}} d\beta d\omega.$$

Define

$$Q_k(\omega, x) := \int_{-1}^{1} q_k(\beta) H_k(\omega, \beta) e^{-j(\omega+k\omega_o)\frac{x\beta}{c}} d\beta,$$

$$-M \le k \le M.$$

So,

$$y(x,t) = \sum_{k=-M}^{M} e^{jk\omega_o t} \frac{1}{2\pi} \int_{-\omega_o/2}^{\omega_o/2} e^{j\omega t} Q_k(\omega, x) d\omega$$

$$= \sum_{k=-M}^{M} e^{jk\omega_o t} L_k(t,x).$$

Since $L_k(t,x)$ is bandlimited to $[-\omega_o/2, \omega_o/2]$, for each k, $-M \le k \le M$, $L_k(t,x)$ can be uniquely determined. Fourier transform of $L_k(t,x)$ with respect to t yields $Q_k(\omega, x)$.

Note that

$$Q_k(\omega, x) = \int_{-1}^{1} q_k(\beta) H_k(\omega, \beta) e^{-j(\omega+k\omega_o)\frac{x\beta}{c}} d\beta .$$

For each fixed $\omega \in [-\omega_0/2, \omega_o/2]$, $Q_k(\omega, x)$ is a bandlimited function of x,which is estimated at the sensor locations, say

$x = 0,\ \pm d,\ \pm 2d,$ etc., where d is the quarter wavelength.

For each fixed ω, $Q_k(\omega, x)$ is the Fourier transform of $q_k(\beta)H_k(\omega, \beta)$, and is a bandlimited function of x, the element locations at the array. Thus for each fixed ω, extrapolation with respect to x yields, for each $\omega \in [-\omega_o/2, \omega_o/2]$,

$$q_k(\beta)H_k(\omega, \beta)$$

for every $\beta \in [-1,1]$ where $q_k(\beta) \neq 0$, and $\omega \in [-\omega_o/2, \omega_o/2]$.

Hence $H_k(\omega, \beta)$ is estimated. Note that $q_k(\beta)$ is already known via equation 4.2. Hence , by estimation of $H_k(\omega, \beta)$, we can estimate the bandlimited time-varying target density function.

CHAPTER V

IMPLEMENTATION OF THE ALGORITHM

The purpose of this thesis is to demonstrate the use of bandlimited extrapolation in the algorithm described in the previous chapter. The equipment used was a Pentium 60 Mhz processor running MATLAB V4.2. The algorithm was implemented in MATLAB's own programming language as a set of sequential steps. The steps are described below. The problems we are faced with can be formulated as below.

a. The signals received by the sensors in the receiving array represent the sum of the reflectivities of all points in the target space. From this, it is required to separate out the individual contributions of each point in the target space.

b. The signal is observed for a very short time and from the behaviour of the target in that time, we are required to estimate its possible behavior outside the observed time range. The information that the movement of the target can be represented by a bandlimited function is assumed.

5.1 The sequential steps of the algorithm

The following is an explanation of the block diagram given in Figure 5.1. This algorithm is proposed to solve the problems described above.

i. From every range and angle, the total signal returned to the sensor element at distance x to the phase center is y(x,t), after the initial round trip time to all the

targets in the range interval $[0, R_1]$, at every angle. The required signal was generated for eleven different sensor locations each spaced d meters apart. The equation used to generate the data received by each sensor location was generated from equation 4.5. The continuous integrals in the formula were approximated by discrete sums. From equation 4.3, the range of the system was calculated and was found to be on the order of 10 Kmeters. The carrier frequency was taken to be 100Mhz and the PRF to be 100 Khz. d, which is the quarter wavelength spacing was set to be 0.185 meters. M is set to be 5. k was chosen to be 10, thus implying that the transmitted signal's bandwidth is around 1Mhz.

ii. It was proven that y(x,t) is a signal of the form

$$y(x,t) = \sum_{k=-M}^{M} e^{jk\omega_0 t} L_k(t,x),$$

where

$$\omega_o = 2\pi \, x \, PRF \ ,$$

and $L_k(t,x)$ is bandlimited to $[-\omega_o/2, \omega_o/2]$.

iii. $L_k(t,x)$ was observed for some time duration of length T_1, at the sensor located at x. One technique that gives us the various $L_k(t,x)$s is amplitude demodulation corresponding to a carrier of frequency $k\omega_0$ yields $L_k(t,x)$. This was done using the demodulating function in MATLAB. The demodulation was repeated for all the values of k. T_1 was taken to be 20 samples.

iv. Extrapolation with respect to t yields $L_k(t,x)$ for all t. This is the first use of the Papoulis-Gerchberg algorithm.This is done for each k, $-M \le k \le M$, for each x in the array. Hence we are extrapolating from 20 samples to 2000 samples of the signal.

v. For each x in the array for $-M \le k \le M$, $Q_k(\omega,x)$ was obtained as the the Fourier transform of $L_k(t,x)$. It is known that for each $\omega \in [-\omega_o/2, \omega_o/2]$, $Q_k(\omega,x)$ is a band limited function of x. For each fixed ω, $Q_k(\omega,x)$ is known for

$$x = x_i \qquad \text{i =10 in this case.}$$

which is an element location in the array. Values of $Q_k(\omega,x_i)$'s were extrapolated to determine $Q_k(\omega,x)$ for all x, for each k, $-M \le k \le M$.. Since there are 10 sensors we have 10 samples for each value of ω and k.

vi. For each fixed k, $-M \le k \le M$, for each $\omega \in [-\omega_0/2, \omega_0/2]$, the Fourier transform with respect to x was performed, to obtain $q_k(\beta)H_k(\omega,\beta)$.

vii. For each k, $-M \le k \le M$, $q_k(\beta)$ is known . Thus, we obtained

$$H_k(\omega,\beta)$$

for $\beta \in [-1, 1]$, such that $q_k(\beta) \neq 0$, and for $\omega \in [-\omega_o/2, \omega_o/2]$. This is the procedure that compensates for the spread of the beam and the presence of the sidelobes as each direction's return is scaled by the magnitude of the beam in that direction.

viii. $H_k(\omega,\beta)$ yielded

$$\overline{\tilde{H}}(\omega, k\frac{2\omega_o}{c}, \beta) \quad \text{for} \quad -M \leq k \leq M,$$

for each fixed (β,ω) of interest.

ix. For each fixed (β,ω) of interest, $\overline{\tilde{H}}(\omega, w, \beta)$ is a bandlimited function whose samples with respect to w were obtained in step (viii). Extrapolation of these samples, yielded $\overline{\tilde{H}}(\omega, w, \beta)$ as a function of w for $-\infty < w < \infty$, for each fixed ω and β of interest. The extrapolation was from 10 samples to 100.

x. The Inverse Fourier transform with respect to w yielded $\tilde{H}(\omega, R, \beta)$, and so, H(ω,R, β) for $R \in [0, R_1]$, for each (ω,β) of interest.

xi. The Inverse Fourier transform with respect to ω for each (R,β) of interest yielded h(t,R,β) for each $t \in (-\infty,\infty)$, $R \in [0, R_1]$, and $\beta \in [-1, 1]$.

This chapter has described how Dr. Emre's algorithm has been implemented. The next chapter seeks to provide a guide to the results and to draw conclusions from them.

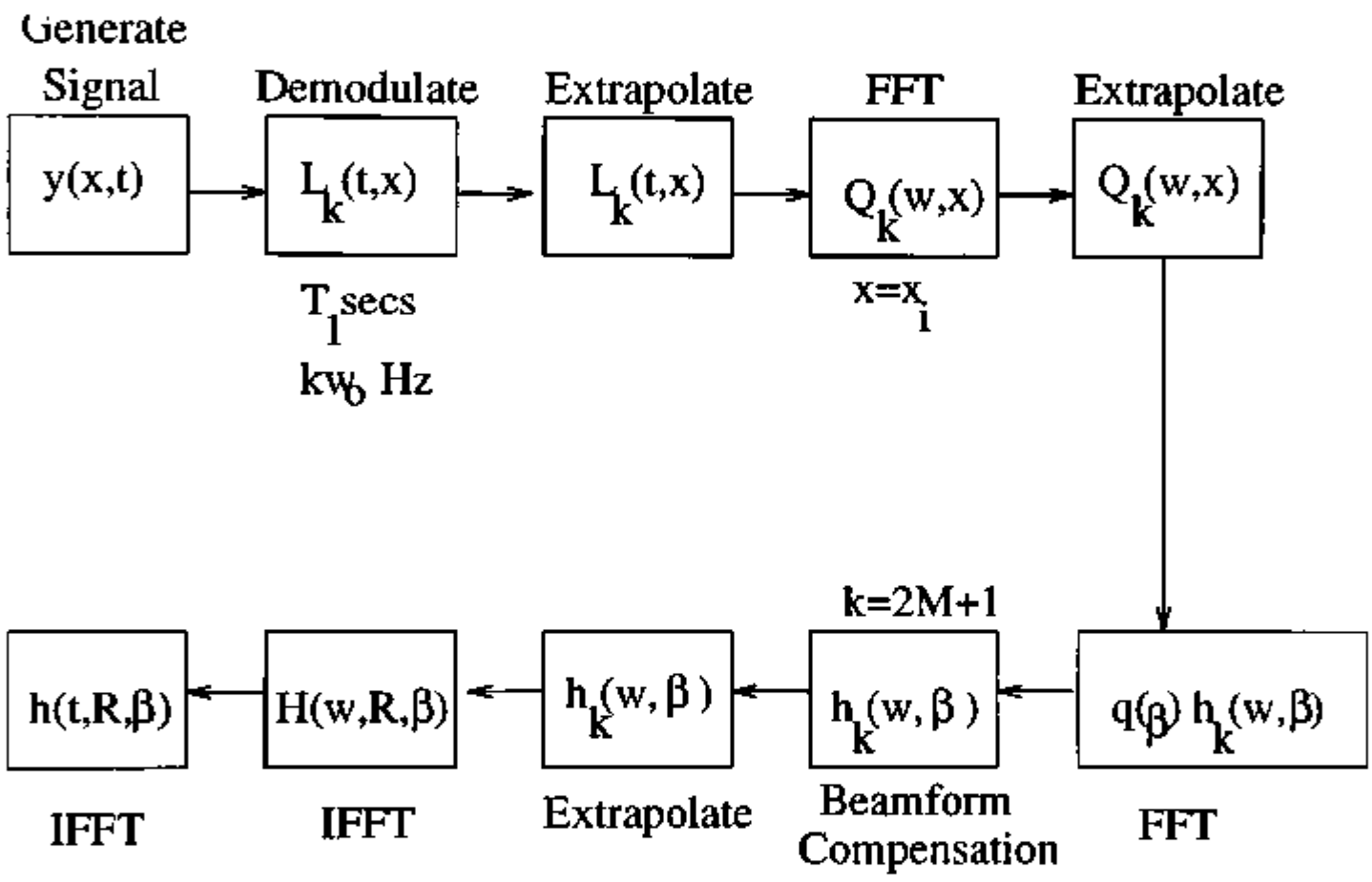

Figure 5.1 Block diagram of Dr. Emre's algorithm

CHAPTER VI

CONCLUSIONS AND RESULTS

The purpose of this chapter is to guide the reader through the graphical comparisons that have been presented as results. The chapter is divided into two parts.

6.1 Results of the Papoulis-Gerchberg algorithm simulations

Four cases are presented wherein, the first figure is a comparison of the original $F(\omega)$, and estimated $F_n(\omega)$, frequency spectra. They are presented as separate graphs because the estimation closely approaches the original. The second figure shows the real and imaginary components of the signal g(t) that have been gated out and are initially available. The third figure consists of comparison graphs of both the imaginary and real parts of the original f(t) and estimated $f_n(t)$ time functions. Now we have achieved the first goal of the thesis which was to verify that extrapolatin was actually done by the algorithm. The fourth figure shows us the convergence curve of the estimation to the original as a function of the number of iterations, thus satisfying the second goal which was to show the effect of the number of iterations on the convergence of the estimate to the original. The fifth figure displays the same albeit for the case where the sampling frequency is double what it was for the displayed functions. A comparison with the original convergence curve gives us an idea of the effect of increasing the sampling rate of the original signal. So,

the third aim of the thesis, that of showing the effect of the sampling rate on the extrapolation has been fulfilled. It is to be noted that displayed functions are shown at the Nyquist frequency.

6.2 Results of the simulations to estimate the Target Density Functions

The first figure shows the comparison between the spectrum of the Target Density Function and its estimate. The estimate is the solid line and the original, the dashed line. This is done in order to satisfy the fourth and fifth goals of the thesis, thereby showing that Dr. Emre's algorithm actuall estimates the time series that represents the Target Density function. The final aim of this thesis has already been extensively covered in Chapter III. Particular importance is paid to the spectrum as compared to the time function. This is because any similarity between the two is more evident here. The time functions for the first two cases, where a symmetric spectrum has been used, show only their real components as the imaginary part is negligible. For purposes of comparison, the plots have been clearly labelled.

6.3 Conclusions and Discussion

The extent of similarity between the estimated and original plots for both sets of results is significant. In the estimation of the Target Density Functions, by inspection we can see that the estimations are similar to passes of the extrapolation algorithm, thus indicating the significant effect the Papoulis-Gerchberg algorithm has

on the final result. The frequency spectra obviously indicate the similarities better than the time functions. We can thus say that the estimation algorithm implemented does actually produce results of a notable accuracy. Real RADAR data would provide us with the actual signal at the sensors. This would greatly increase the accuracy of the estimation, because in this implementation we have worked with already corrupted data. Dr. Emre has also developed another algorithm for performing the same function and this uses the concept of wavelets and promises to be less computing and memory intensive. This is to be explored in the future. A much more detailed exploration of the capabilities of this algorithm for high bandwidth functions would need to be undertaken too, as only very low bandwidths were assumed in this implementation. The following values were taken to be constant throughout the implementations. Real time data from a RADAR installation, if available, may be used to put this algorithm through the final test. As can be seen from the results, this algorithm does merit further investigation and subsequent application in the RADAR field.

The Papoulis-Gerchberg algorithm has been shown to be very effective for bandlimited extrapolation. It has been shown that the algorithm is computationally accurate enough for application in the RADAR signal processing field.

REFERENCES

(1) A. Papoulis, " A New Algorithm in Spectral Analysis and Bandlimited Extrapolation," IEEE Transactions on Circuits and Systems, Vol. CAS, pp 735-742, September, 1975.

(2) E.Emre, " A Summary of certain Extrapolation Techniques in the Presence of Noise," Texas Tech University, March 1994.

(3) E.Emre, " Time-Varying Target Density Function Estimation," Texas Tech University, March 1992.

(4) E.Emre, "Existence of Target Density Functions in Time-Varying Environments," Texas Tech University, March 1994.

(5) E.Emre, "On Aspects of Radar Signal Processing," Texas Tech University, June 1988.

(6) E.Emre, "Estimation and Analysis of Target Density Functions via Wavelet and Gabor Theory," Texas Tech University, March 1994.

(7) E.Emre, " A Report to Texas Instruments," Texas Tech University, Feb 1995.

(8) Gershon J.Wheeler, Radar Fundamentals, Prentice-Hall, Englewood Cliffs, NJ, 1967.

(9) Alan V.Oppenheim and Ronald W.Schafer, Discrete-Time Signal Processing, Prentice-Hall, Englewood Cliffs, NJ, 1989.

(10) Signal Processing Toolbox, MATLAB, 1994.

(11) Simon Haykin, Communication Systems, Wiley, New York,1991.

(12) N. Levanon, Radar Principles, Wiley, New York, 1988.

(13) Edward W.Kamen, Introduction to Signals and Systems, Macmillan, New York, 1990.

(14) E.Emre, " Conditions for the Existence of Time-Varying Target Density Functions," Texas Tech University, April 1992.

APPENDIX A

RESULTS OF THE PAPOULIS-GERCHBERG ALGORITHM

CASE A.1

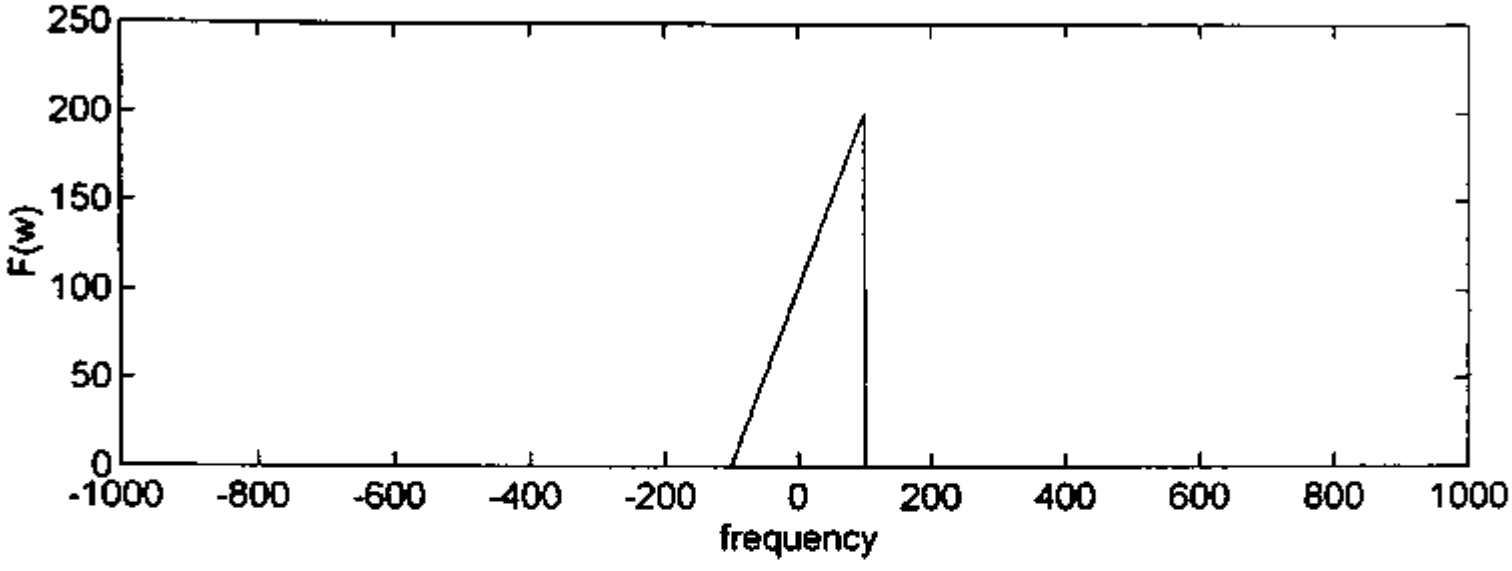

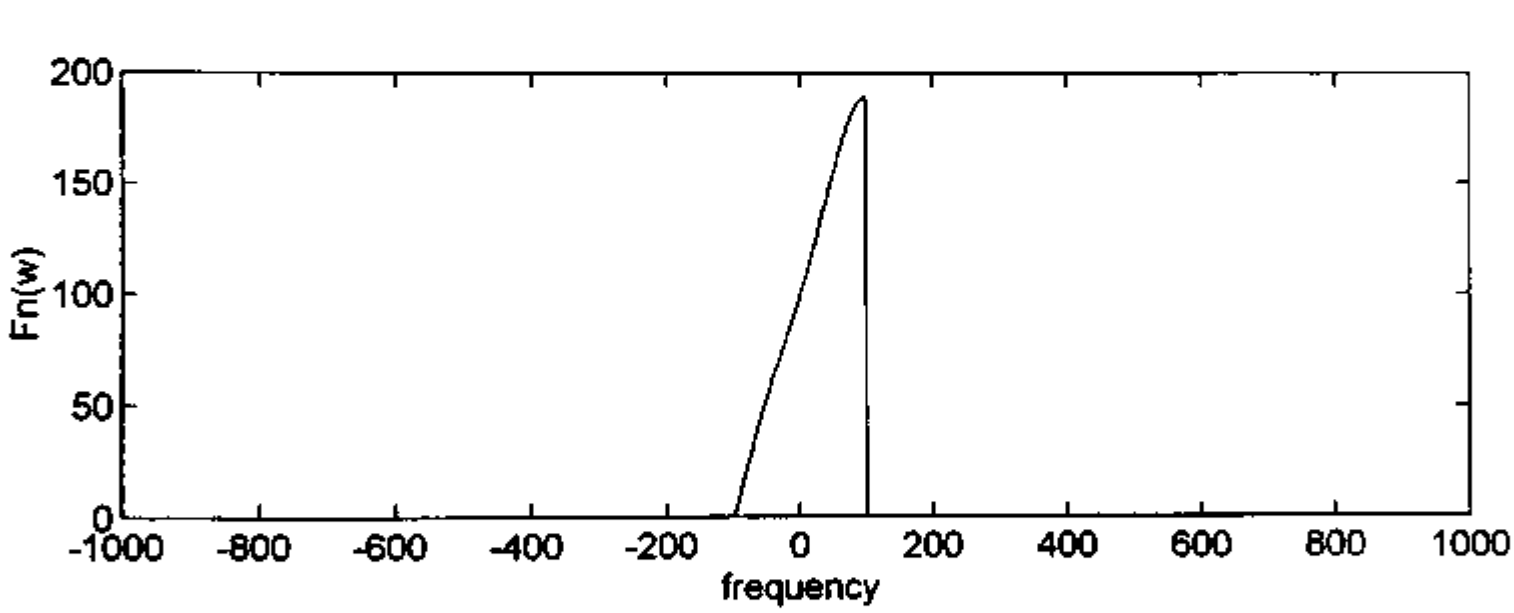

Figure A.1 Results of Case I of the Papoulis-Gerchberg algorithm

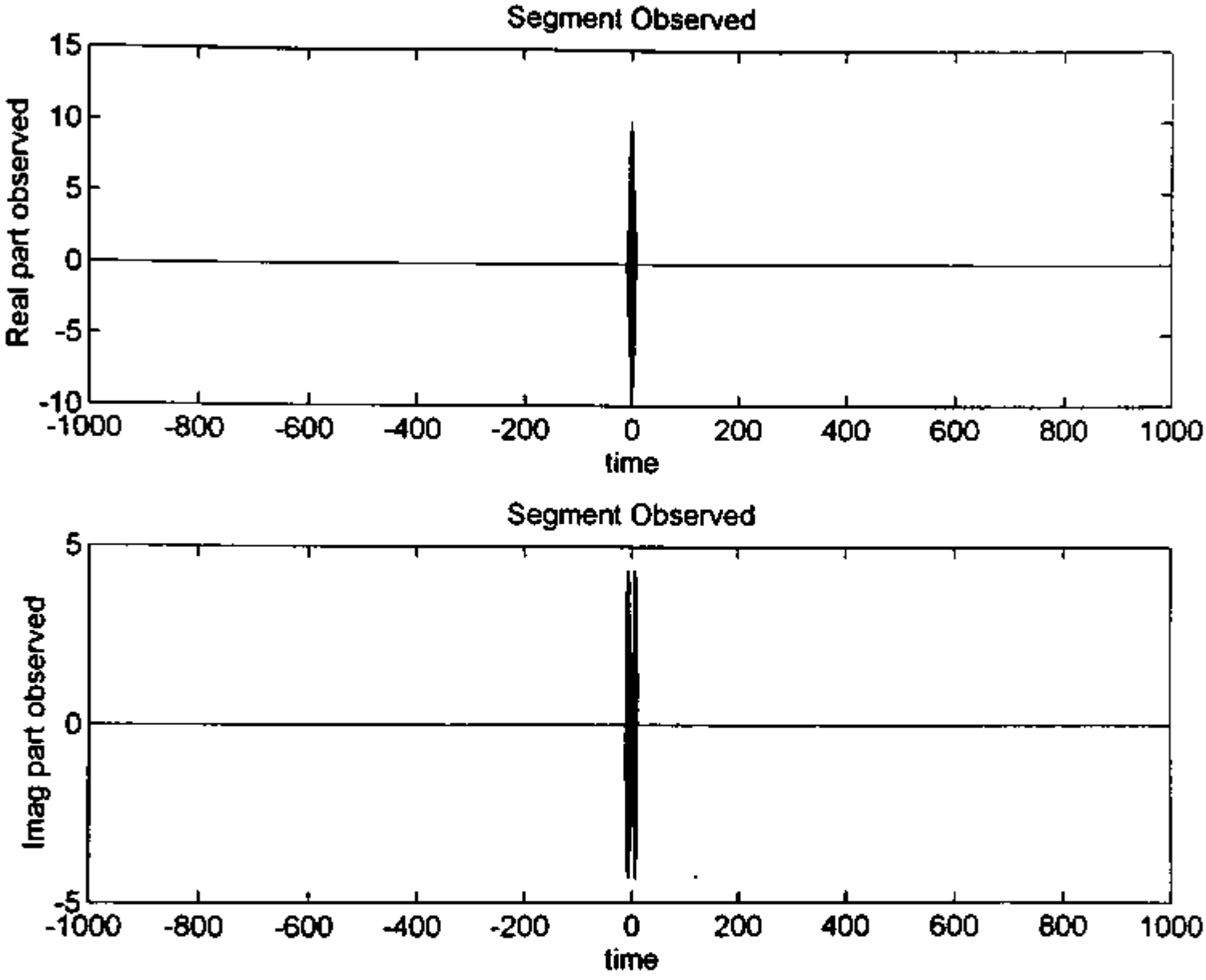

Figure A.1 Continued

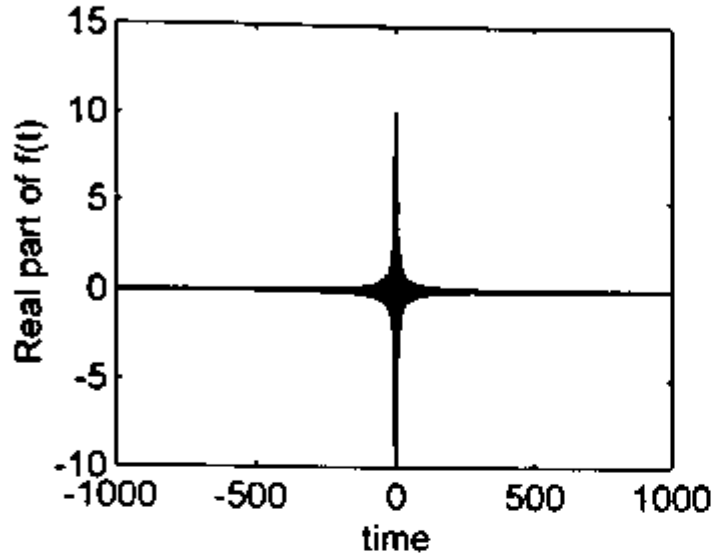

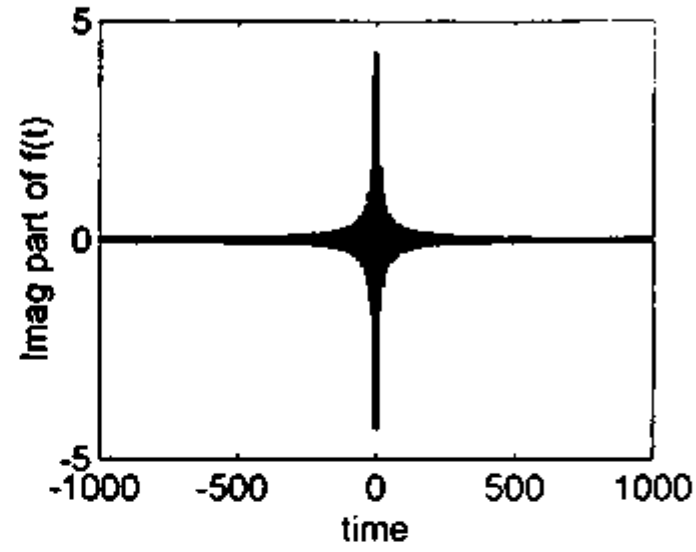

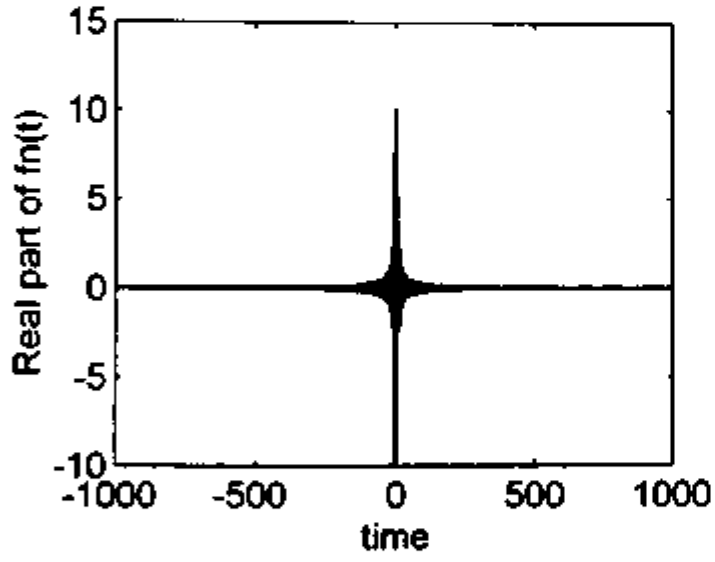

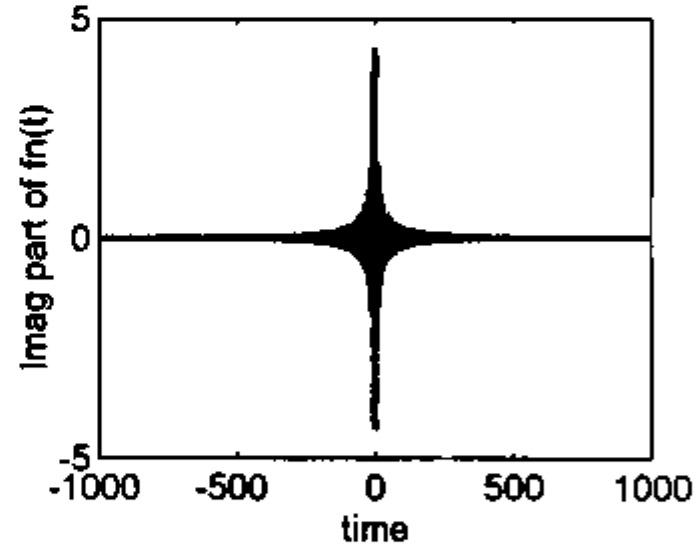

Figure A.1 Continued

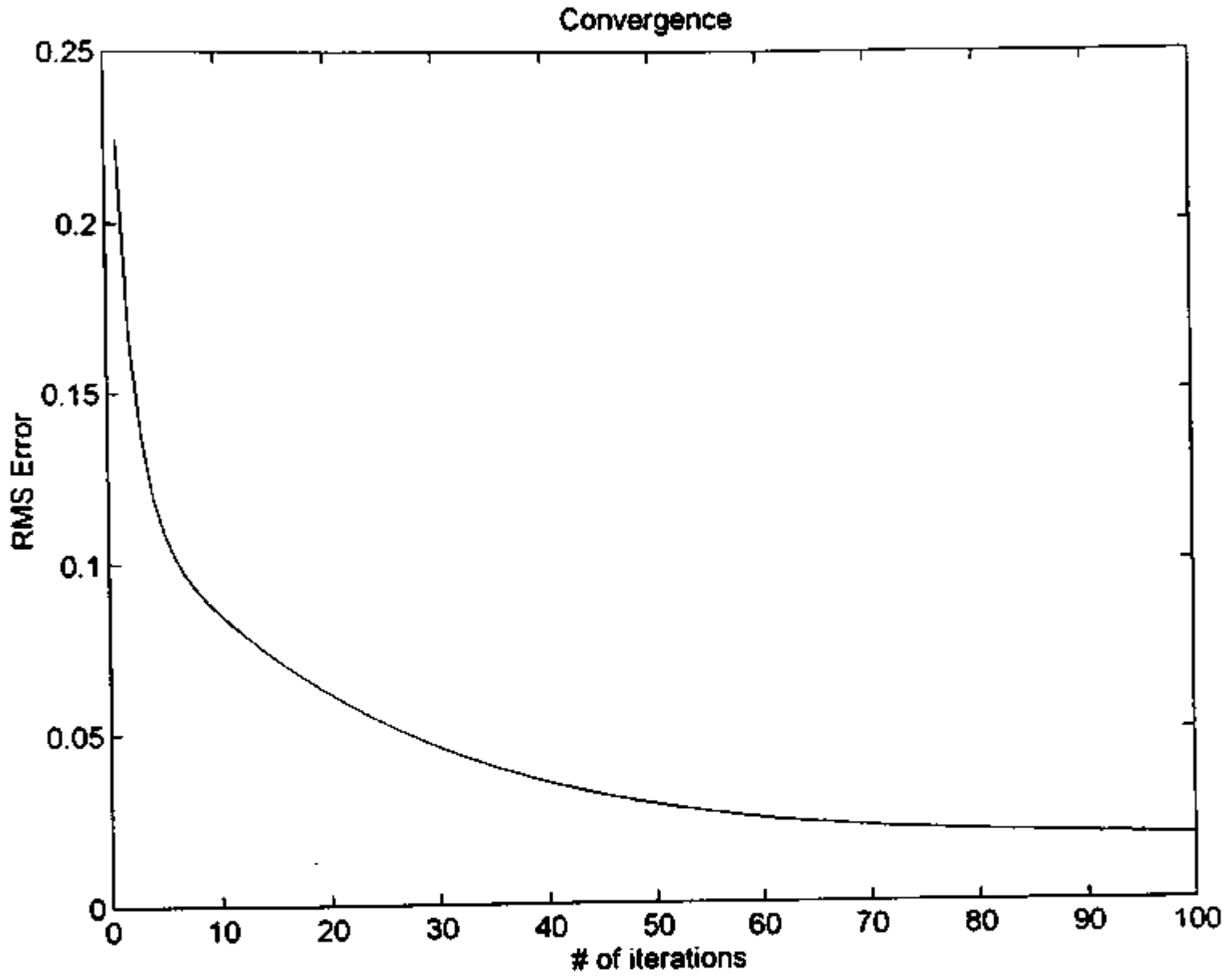

Figure A.1 Continued

CONVERGENCE CURVE FOR THE CASE WITH HIGHER SAMPLING RATE

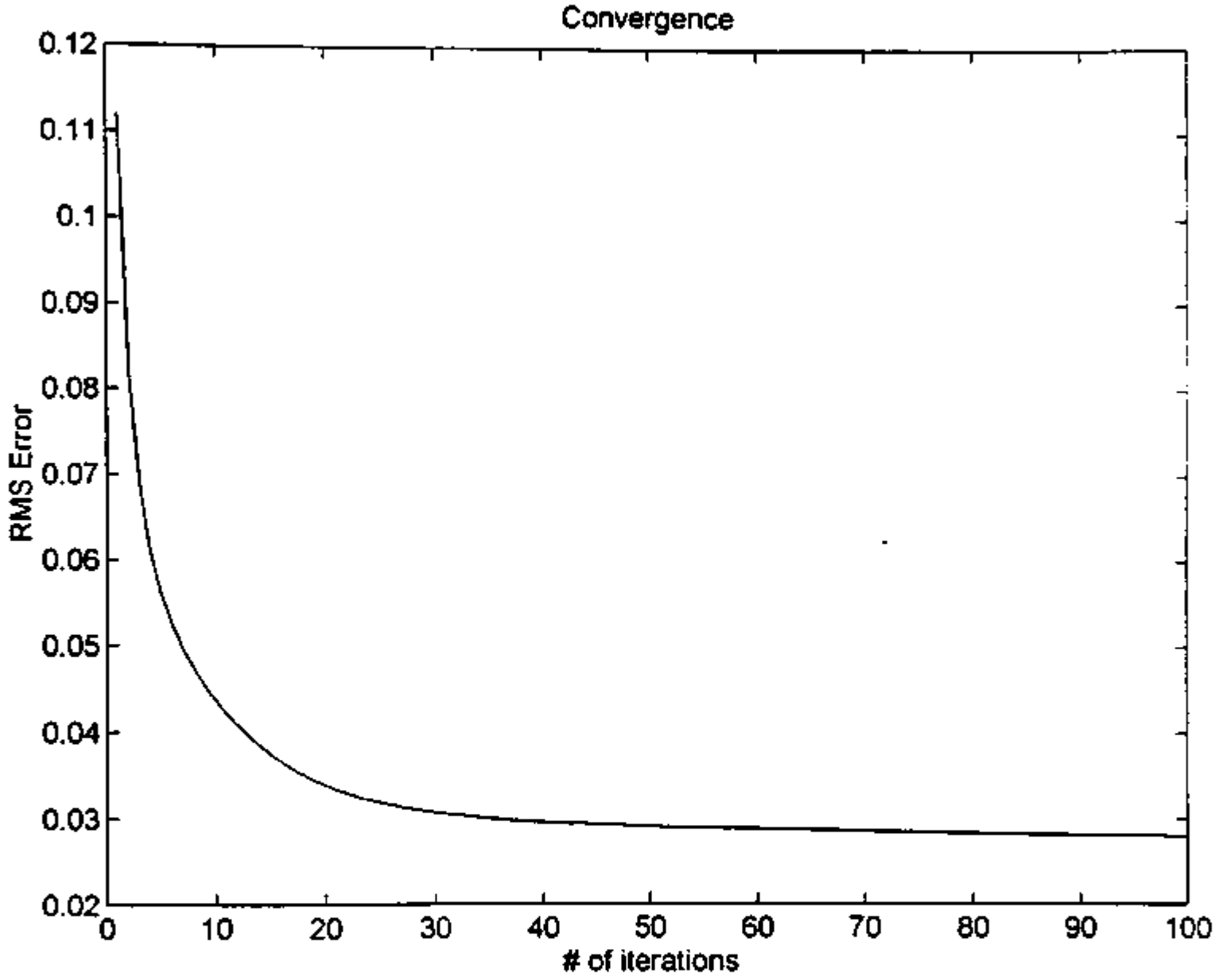

Figure A.1 Continued

CASE A.2

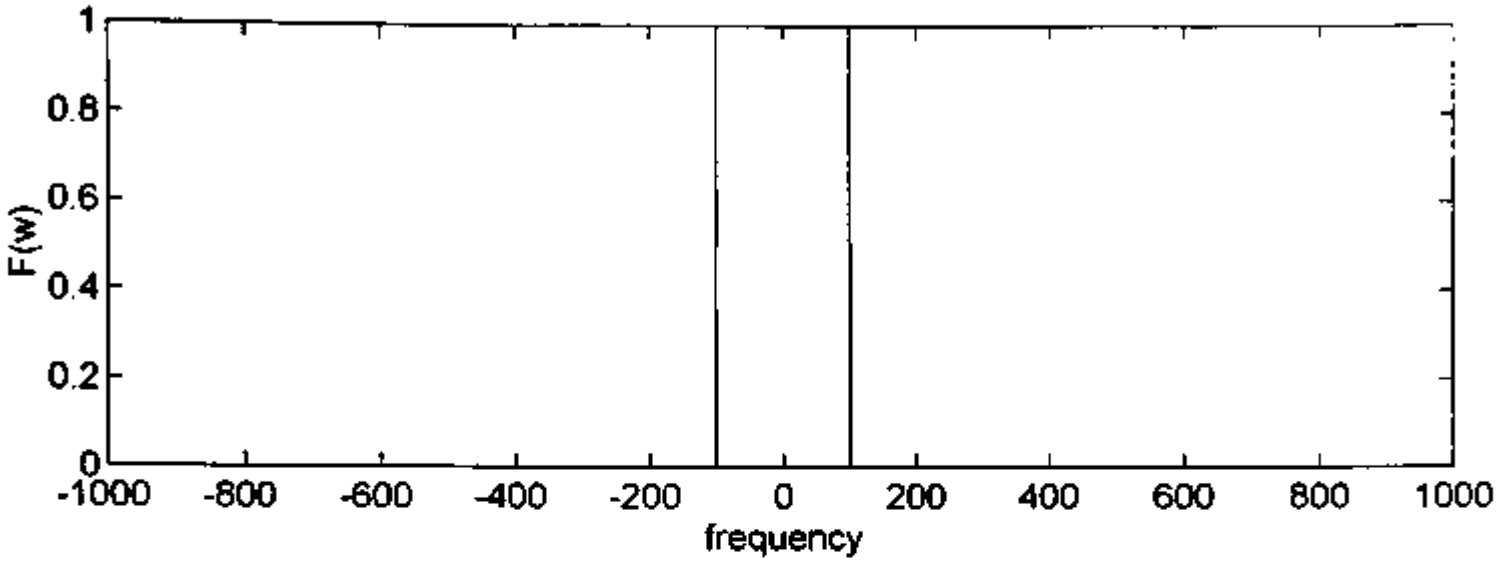

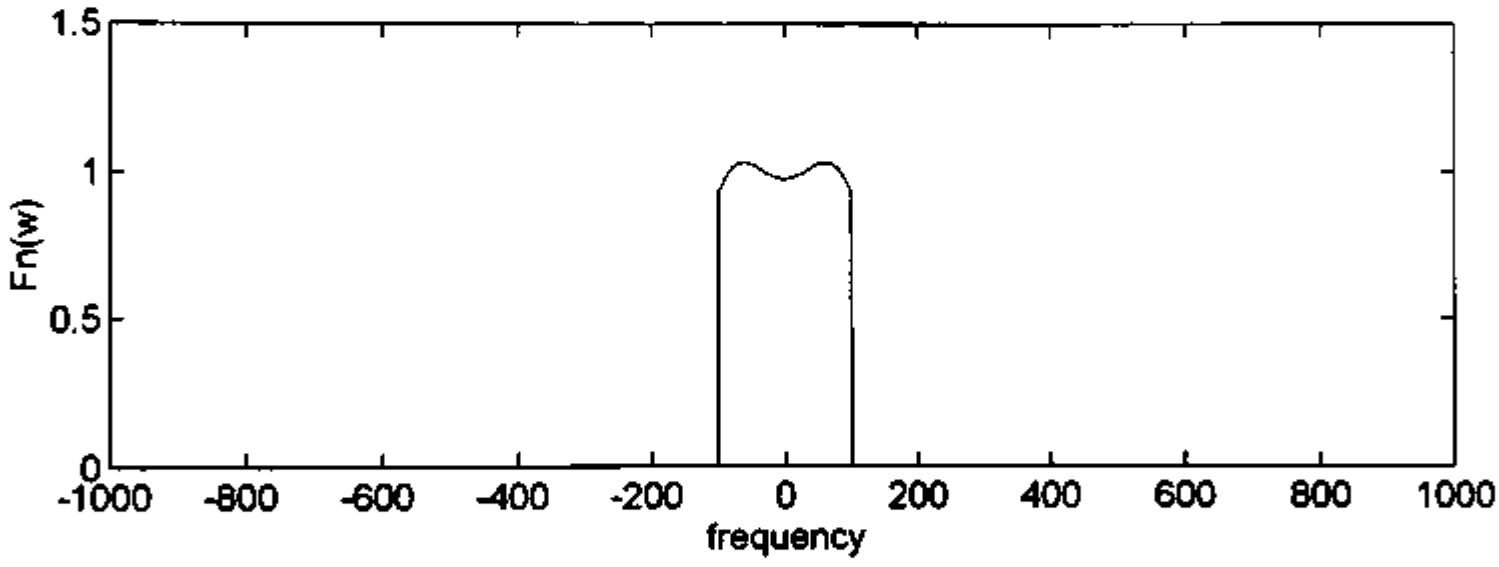

Figure A.2 Results of Case II of the Papoulis-Gerchberg algorithm

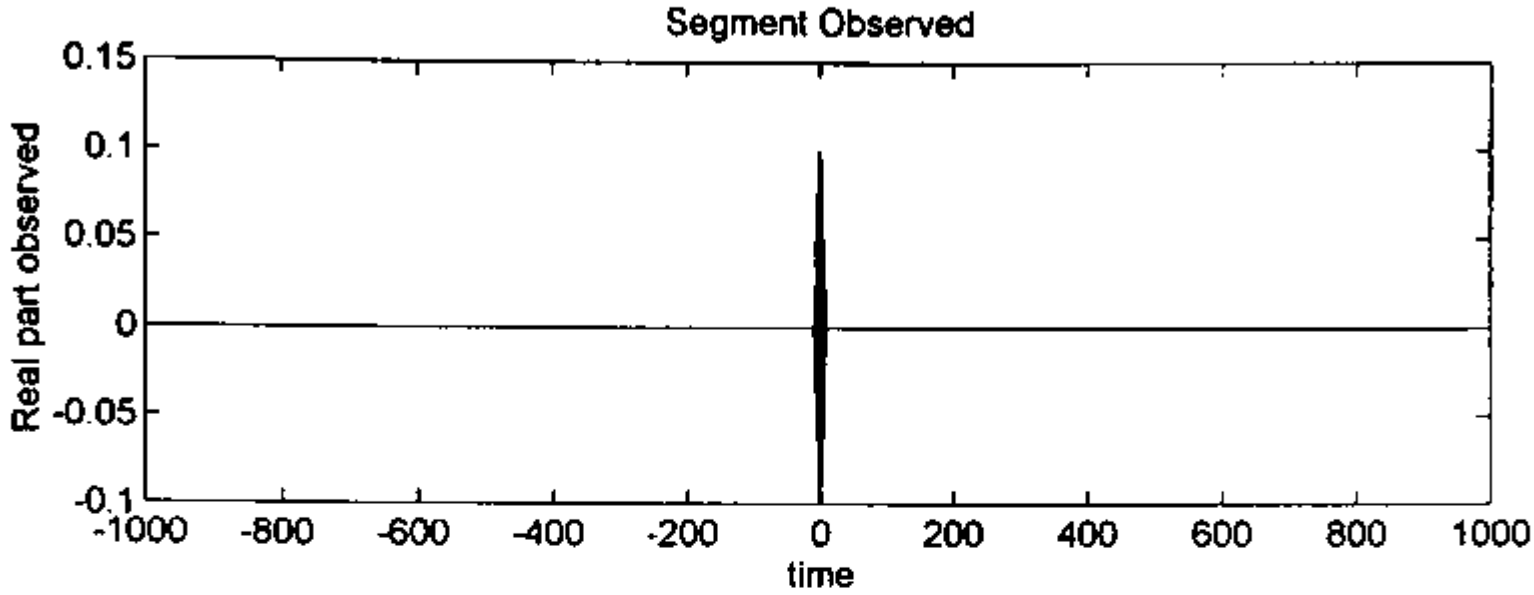

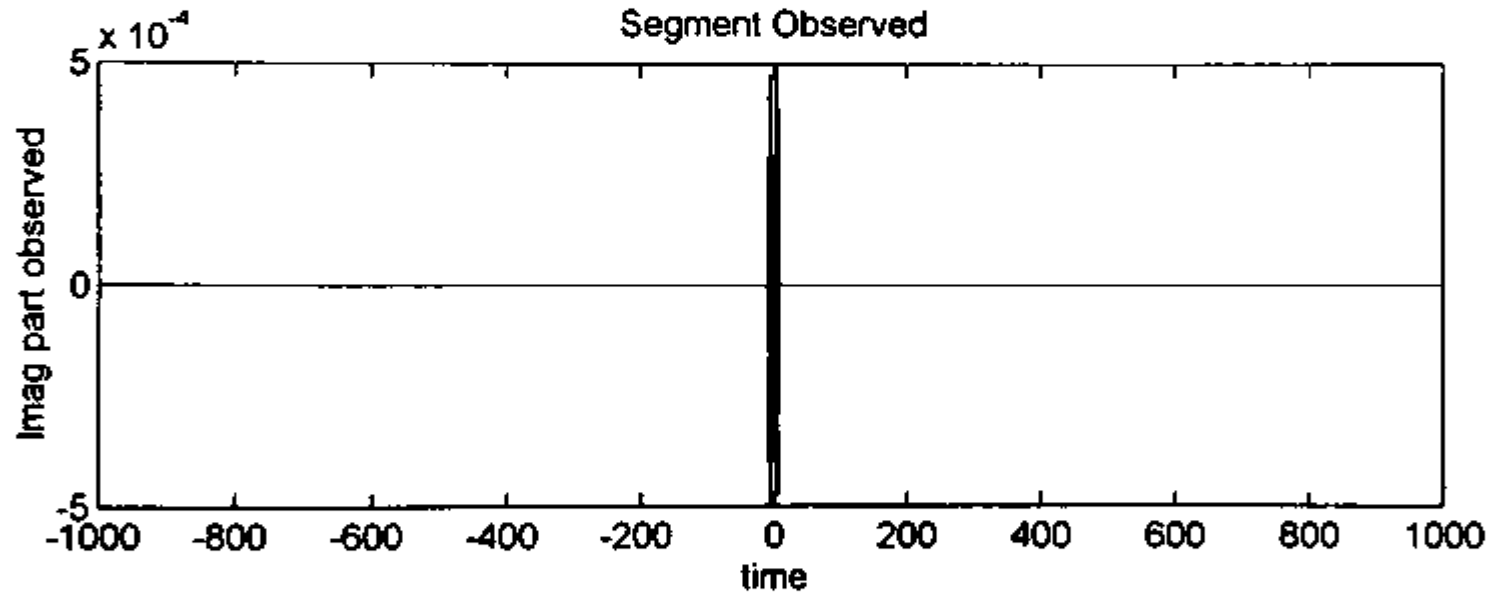

Figure A.2 Continued

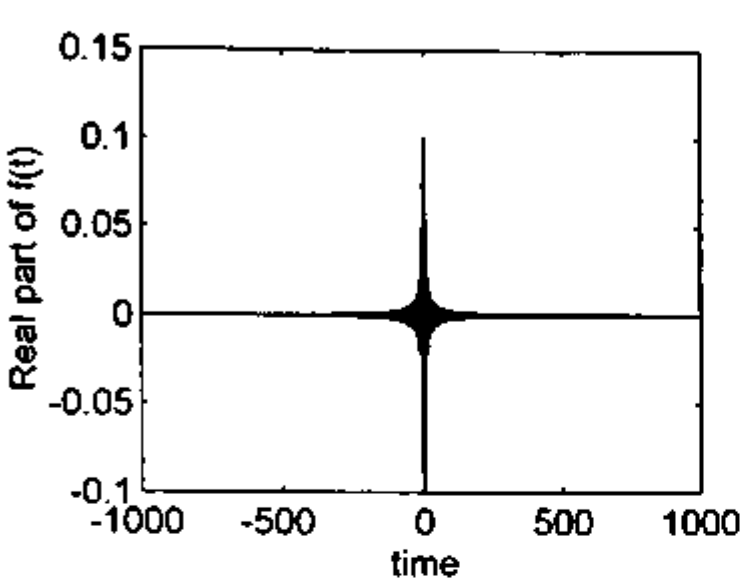

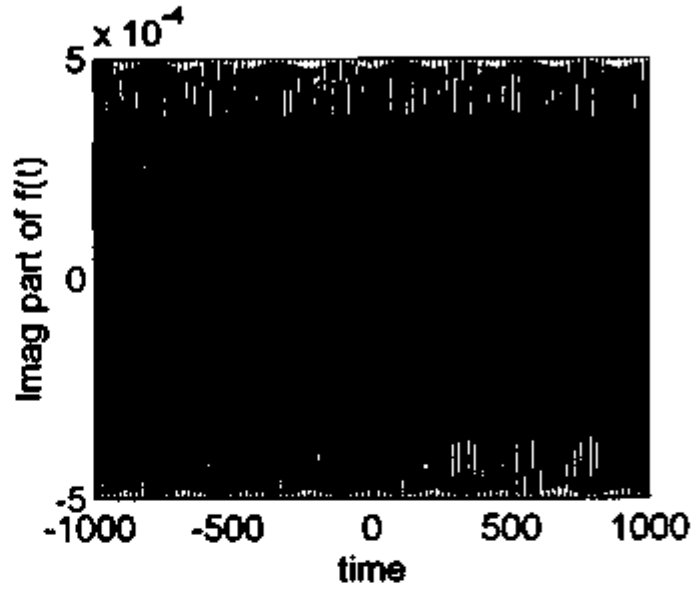

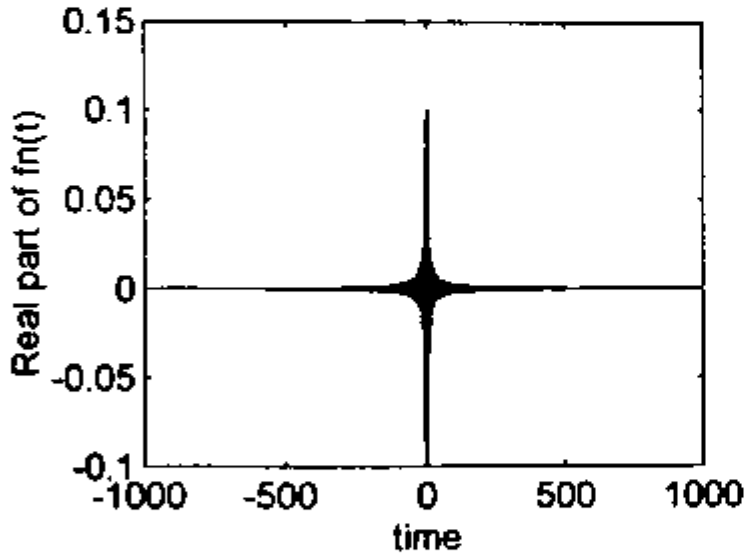

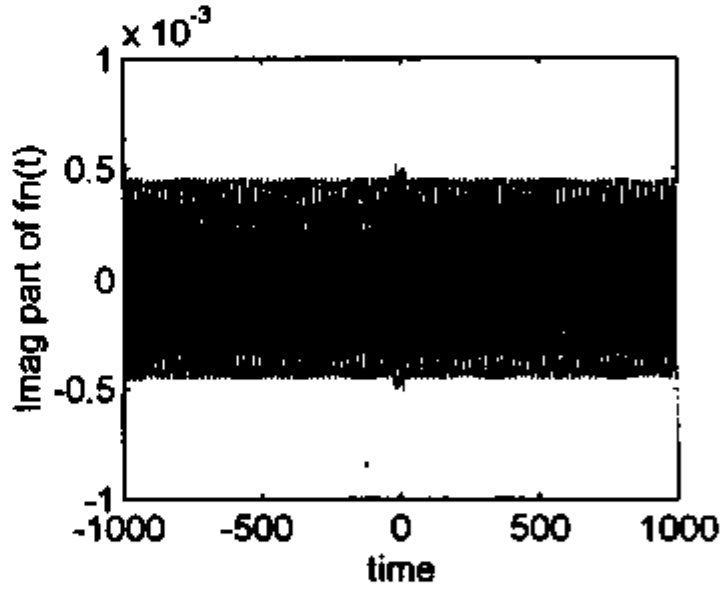

Figure A.2 Continued

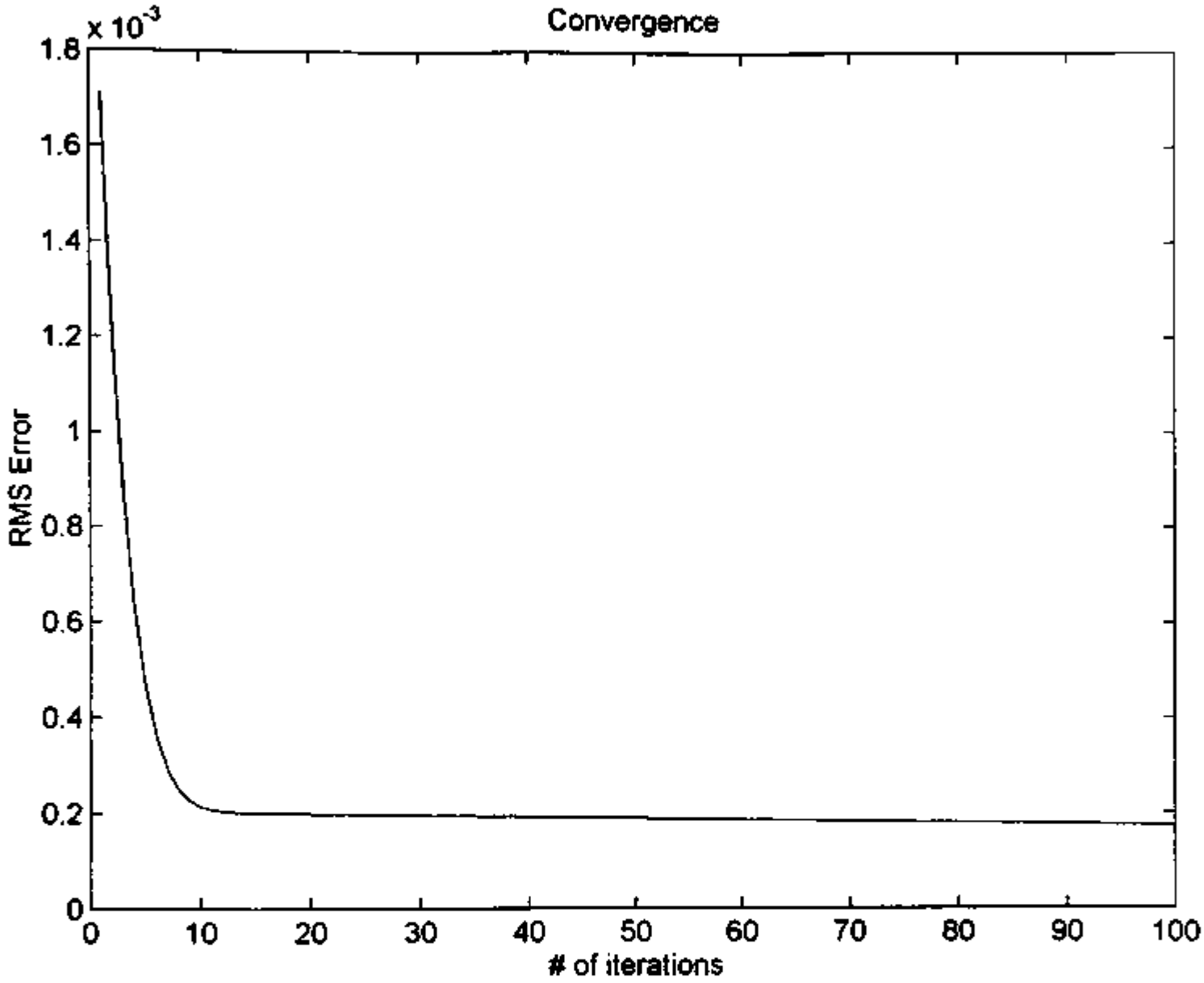

Figure A.2 Continued

CONVERGENCE CURVE FOR THE CASE WITH HIGHER SAMPLING RATE

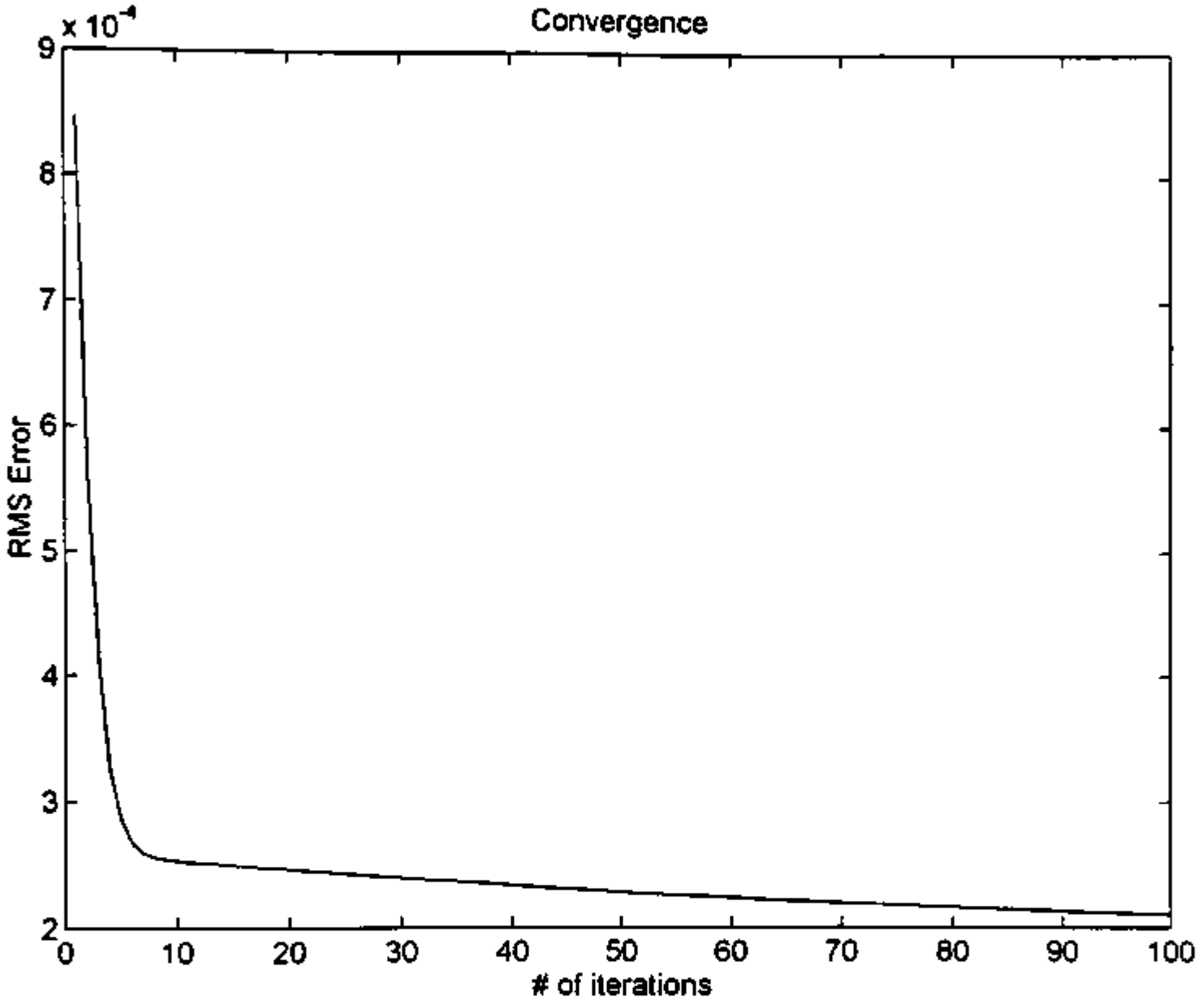

Figure A.2 Continued

CASE A.3

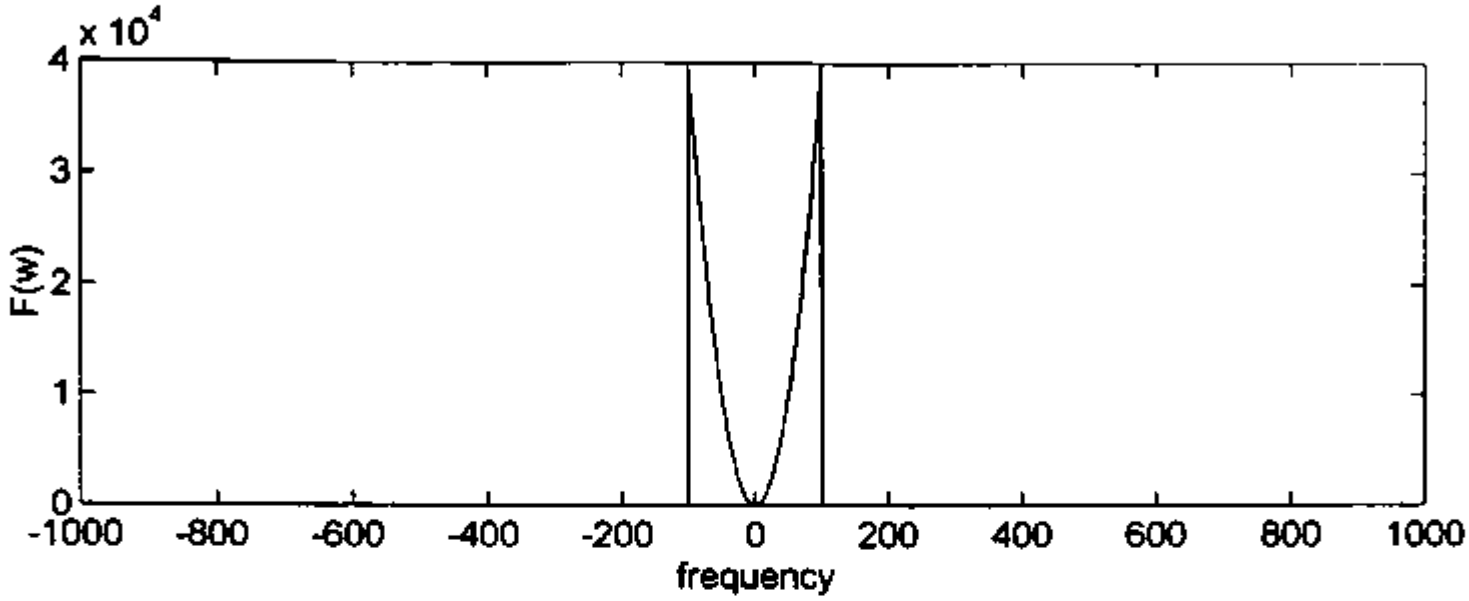

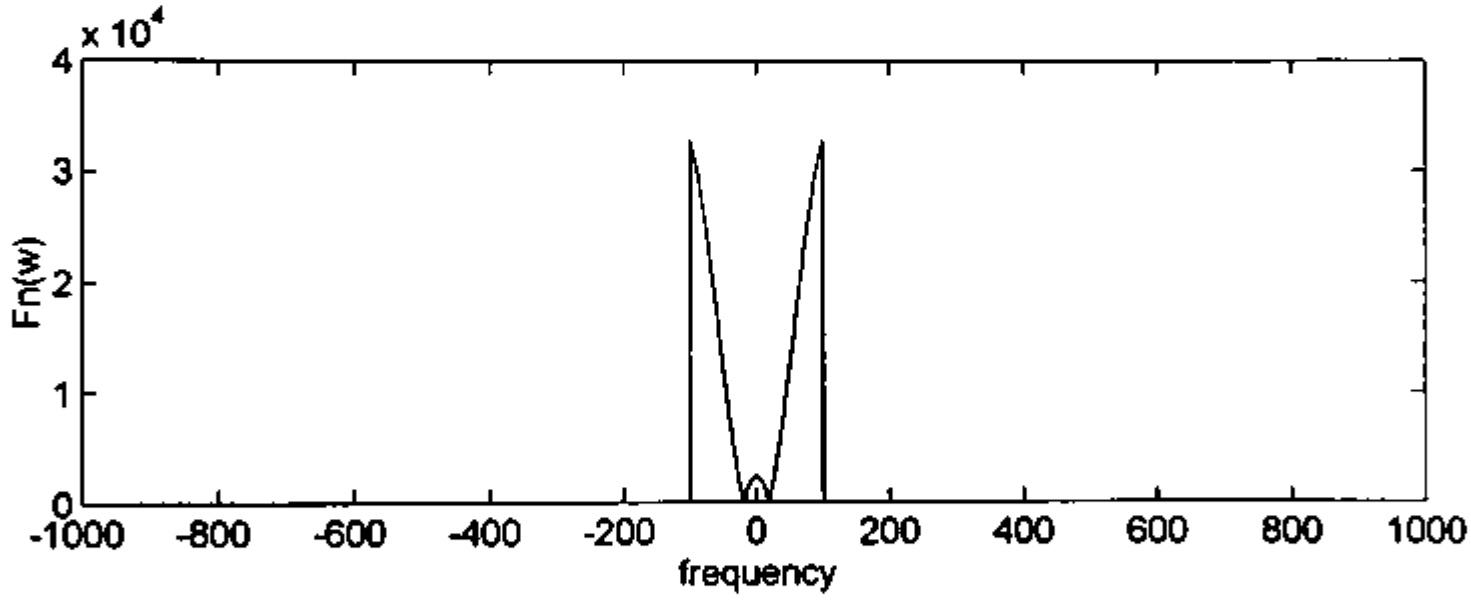

Figure A.3 Results of Case III of the Papoulis-Gerchberg algorithm

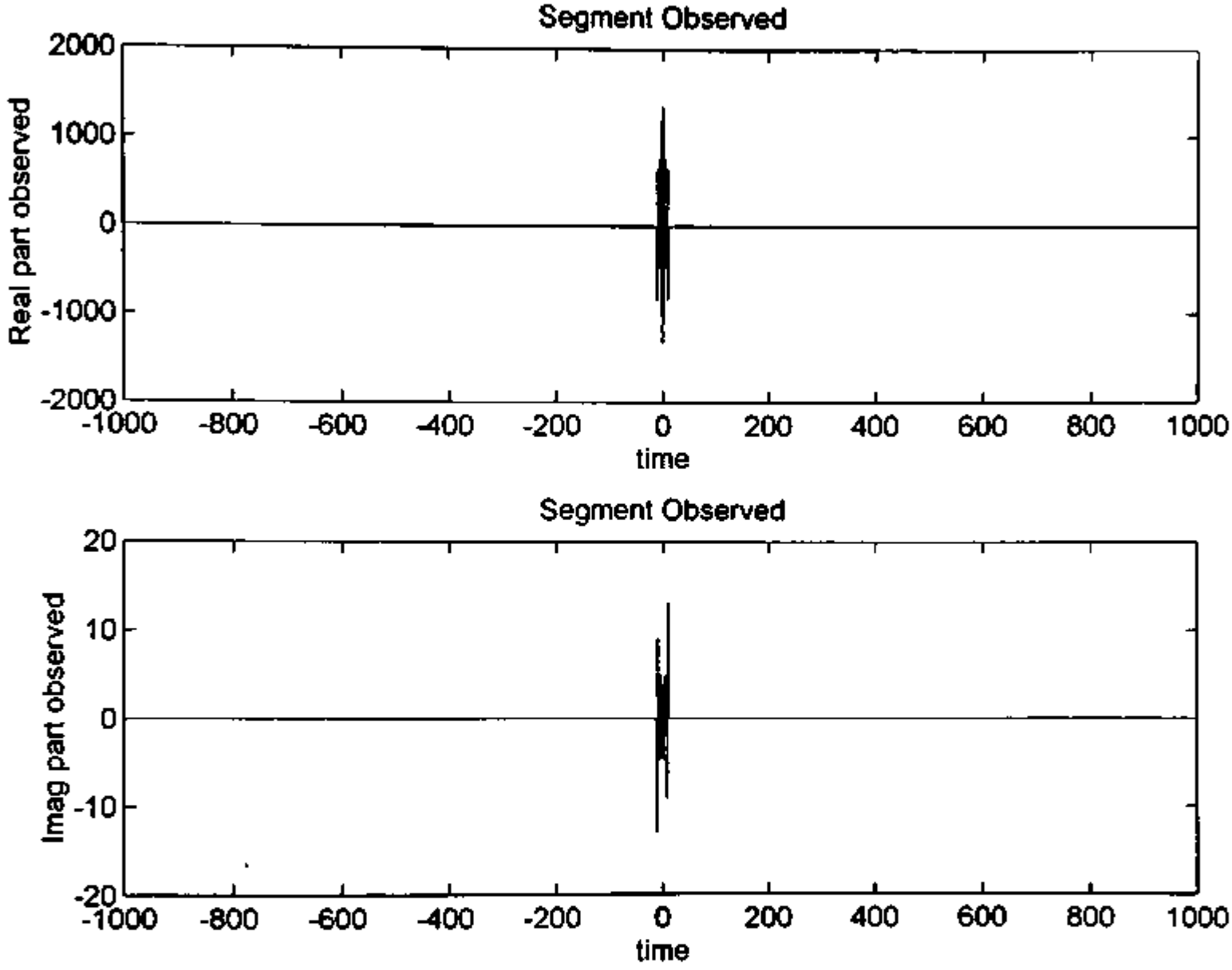

Figure A.3 Continued

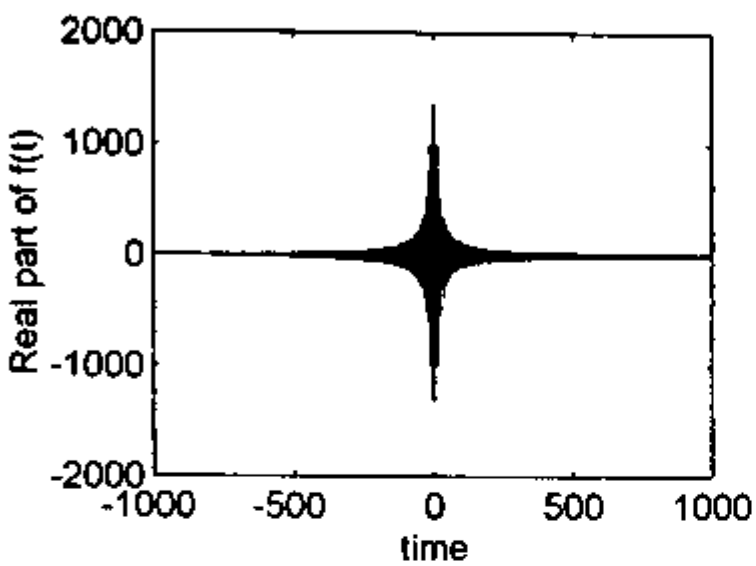

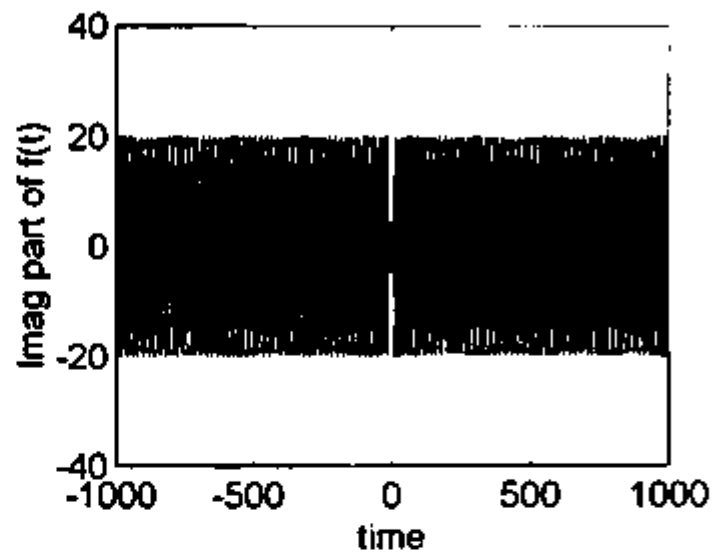

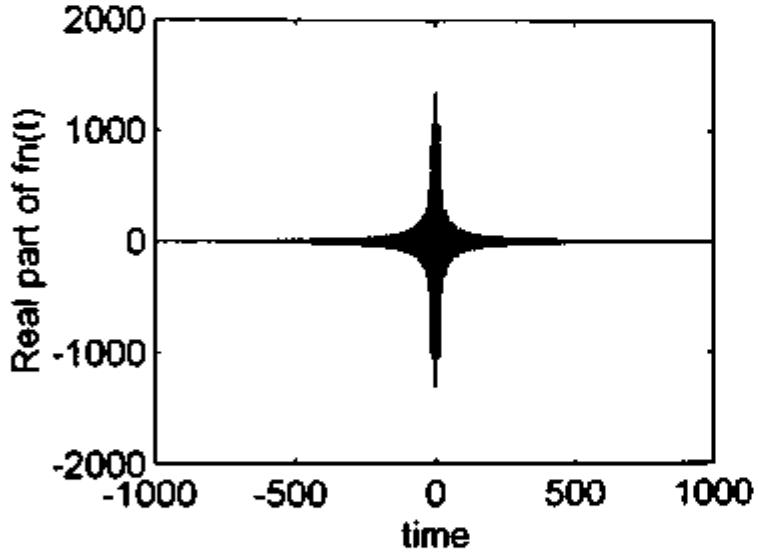

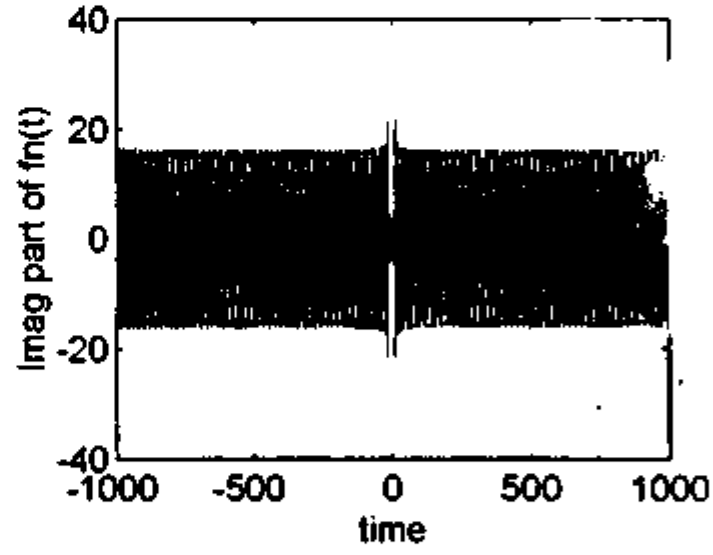

Figure A.3 Continued

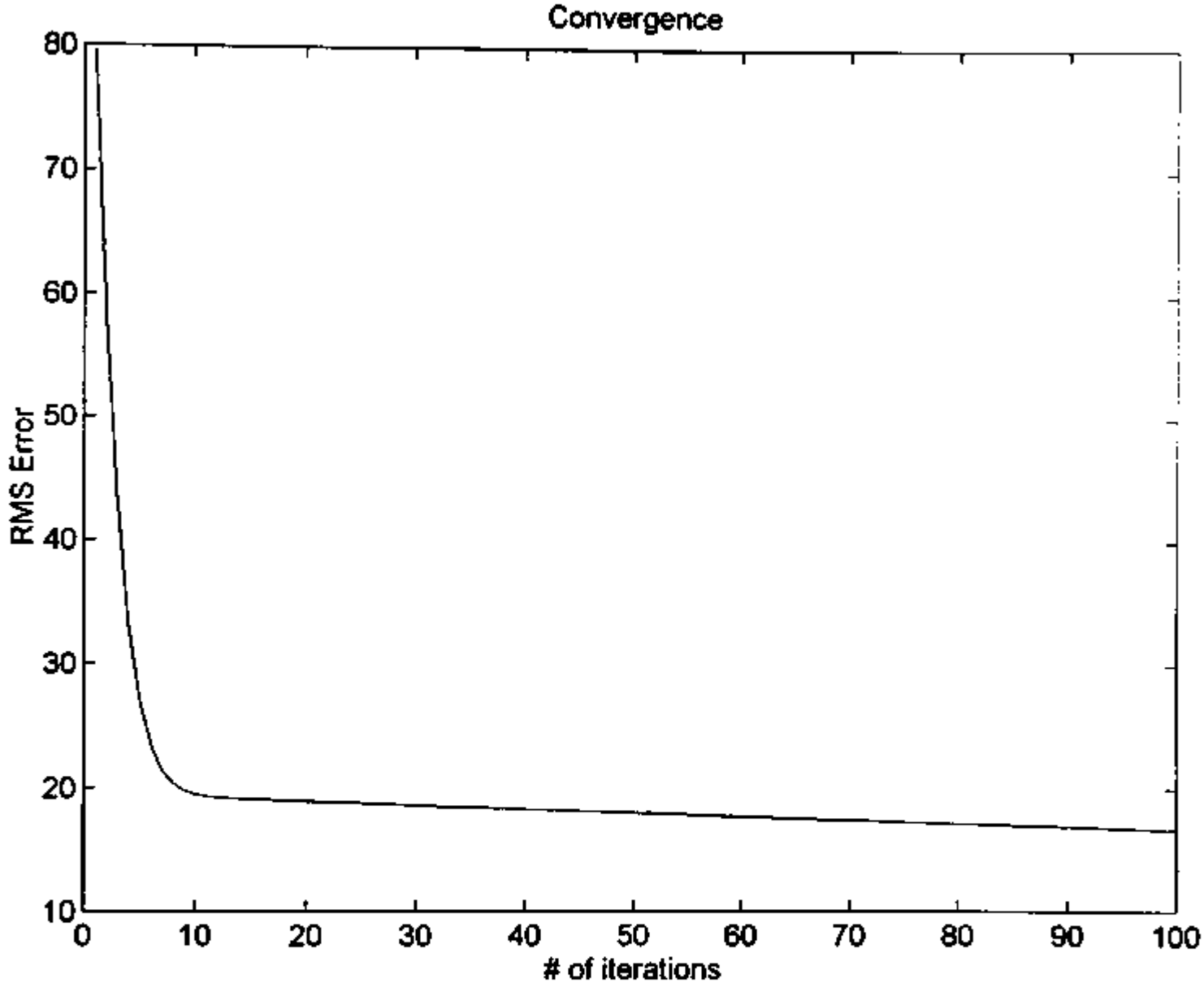

Figure A.3 Continued

CONVERGENCE CURVE FOR THE CASE WITH HIGHER SAMPLING RATE

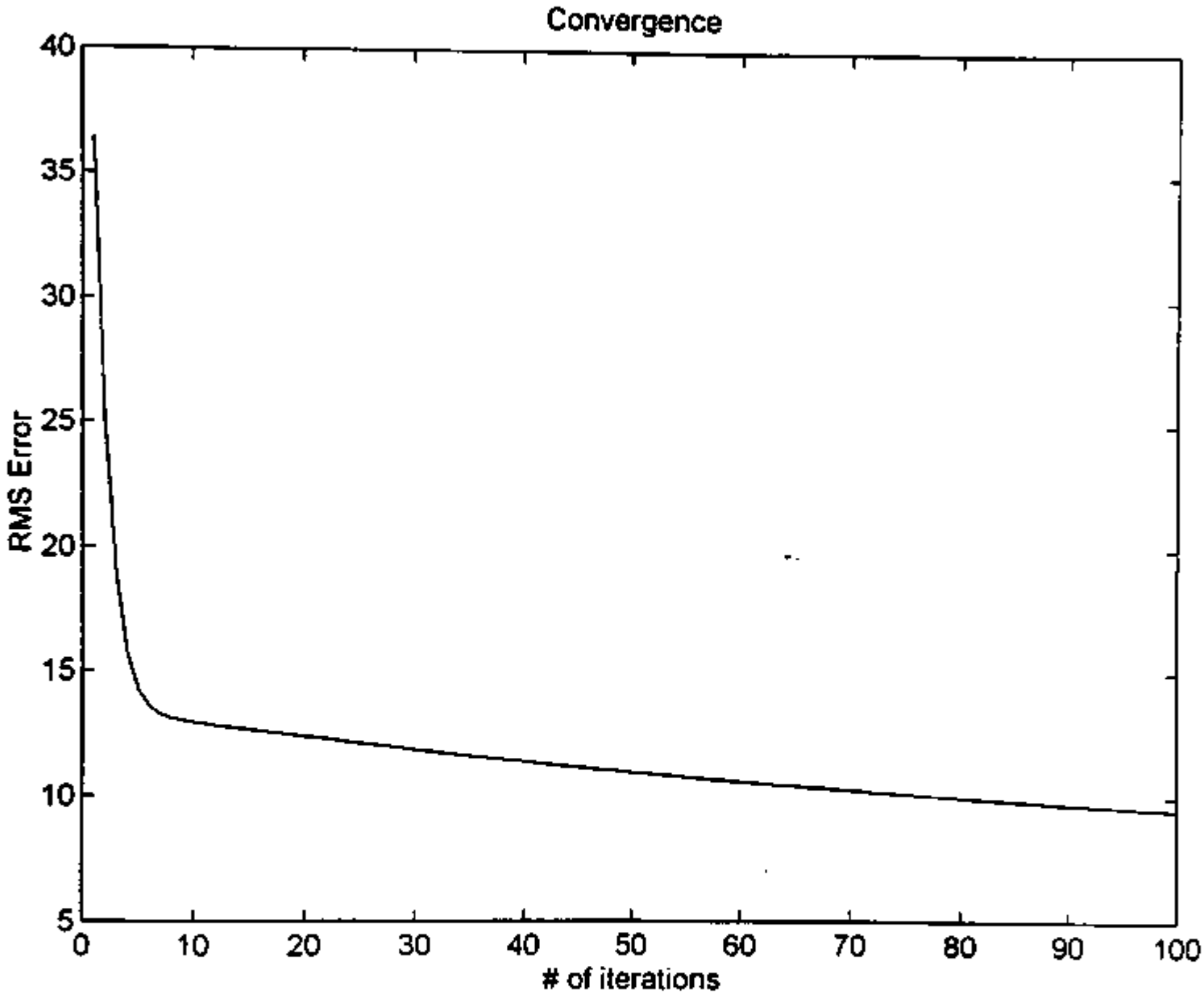

Figure A.3 Continued

APPENDIX B

RESULTS OF TARGET DENSITY FUNCTION ESTIMATION

CASE B.1

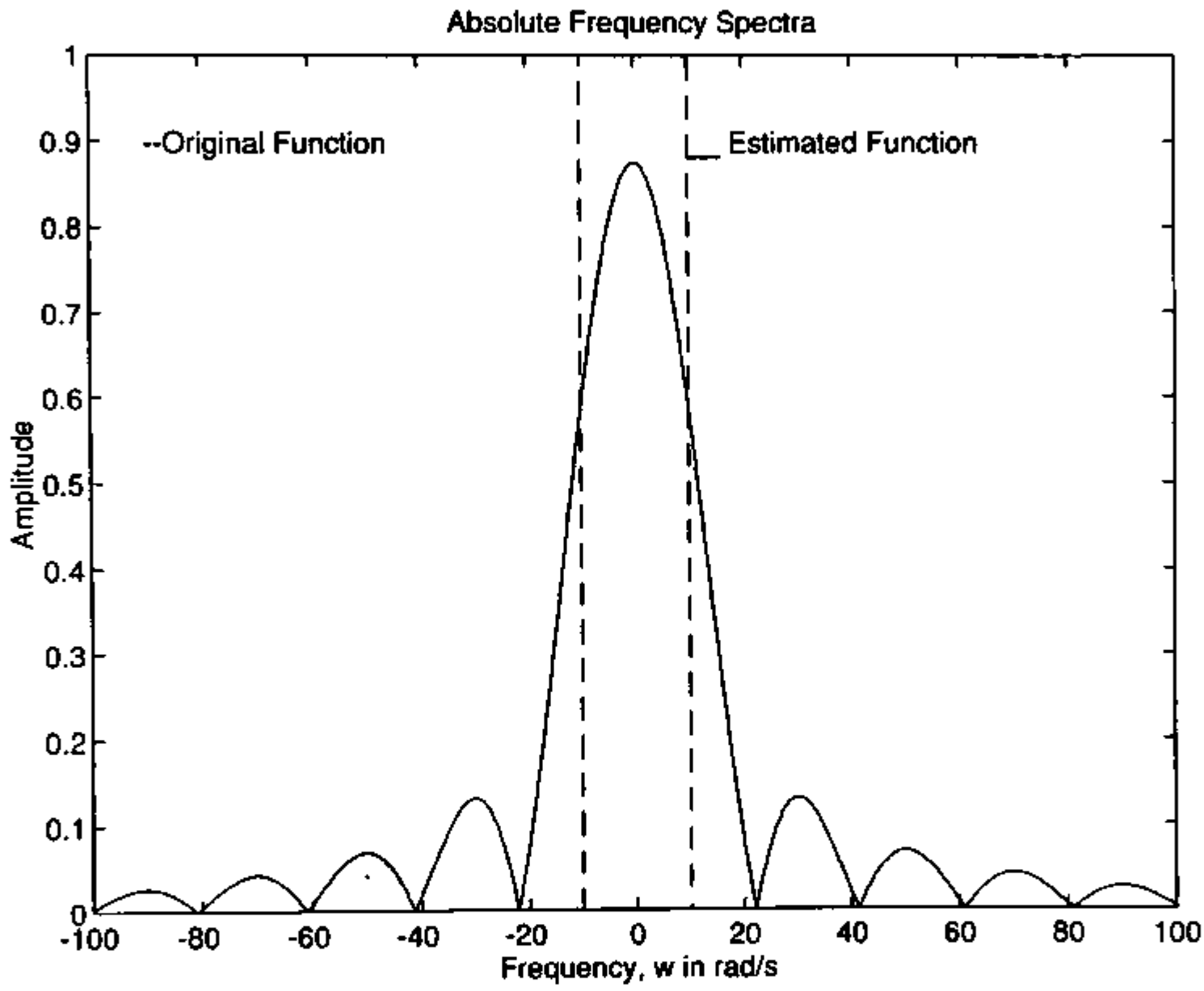

Figure B.1 Results of Case I of Target Density function estimation

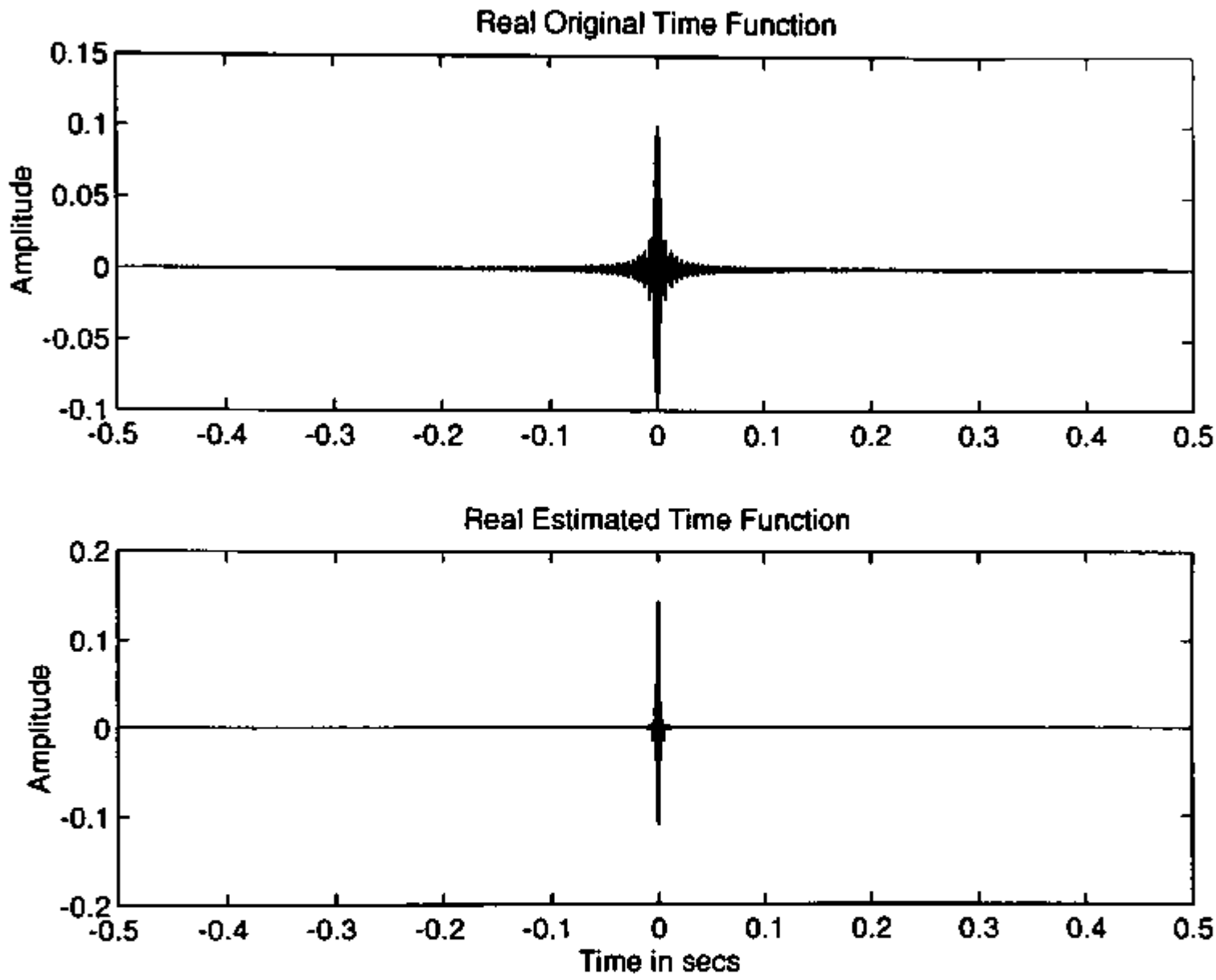

Figure B.1 Continued

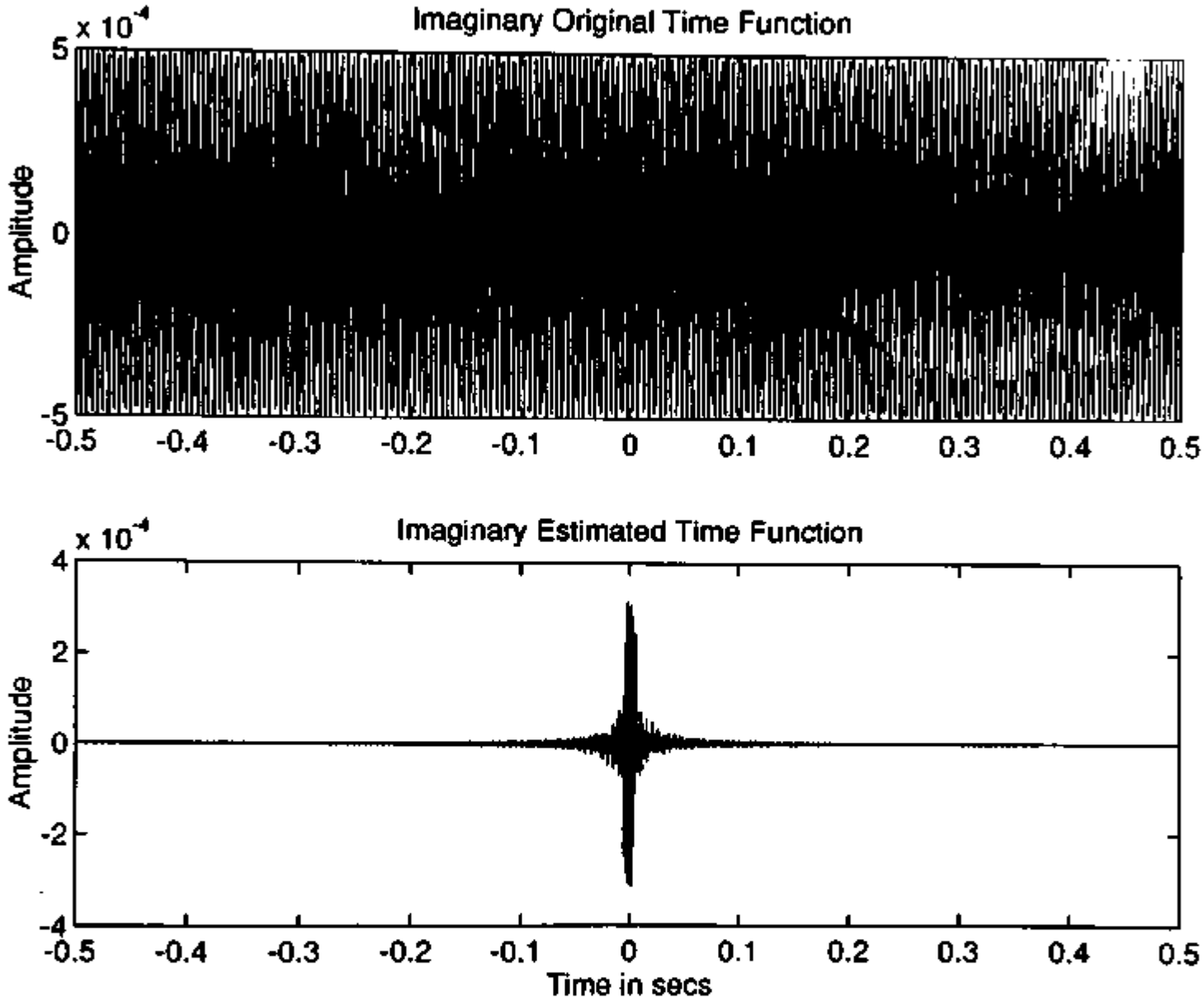

Figure B.1 Continued

CASE B.2

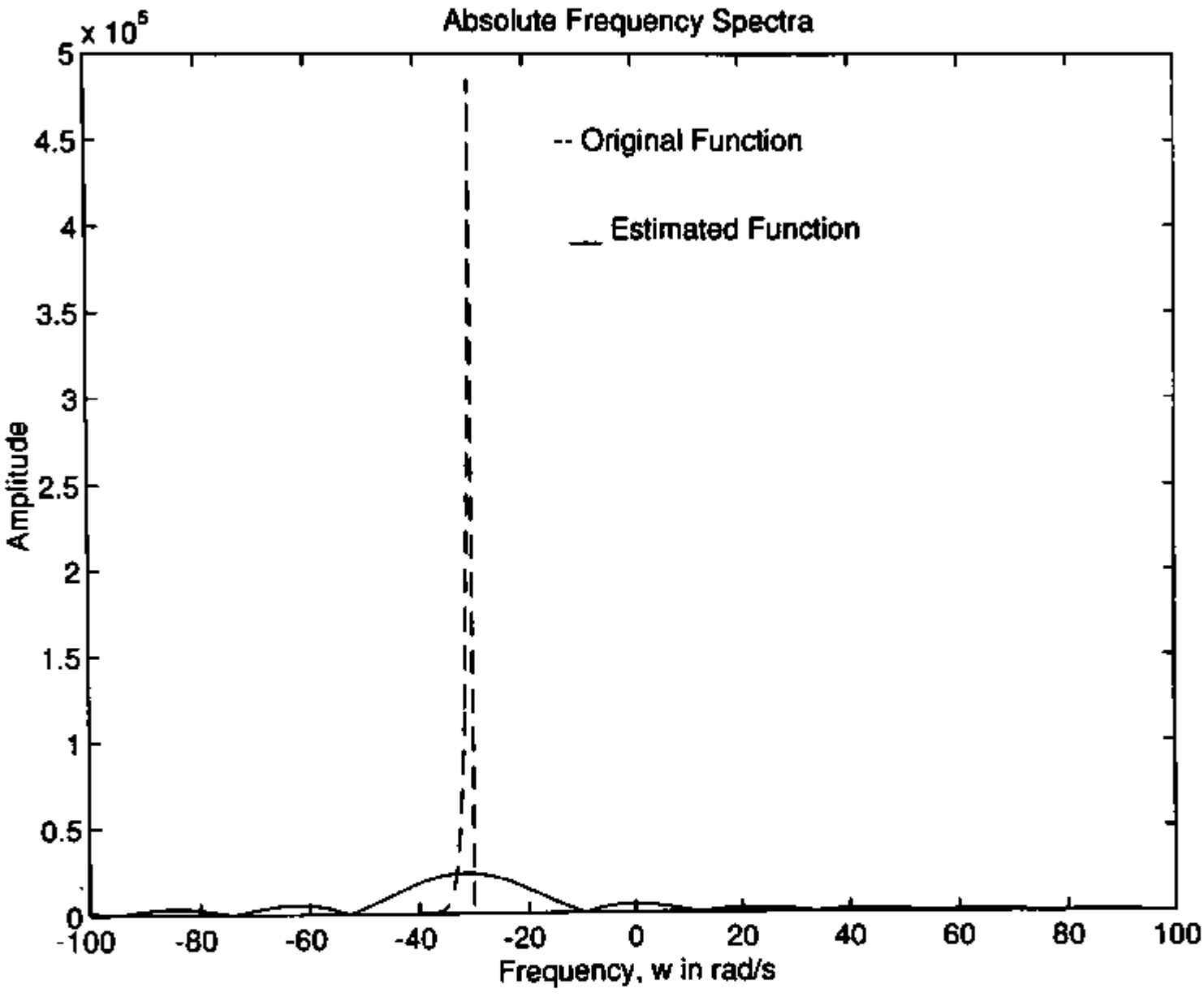

Figure B.2 Results of Case II of Target Density function estimation

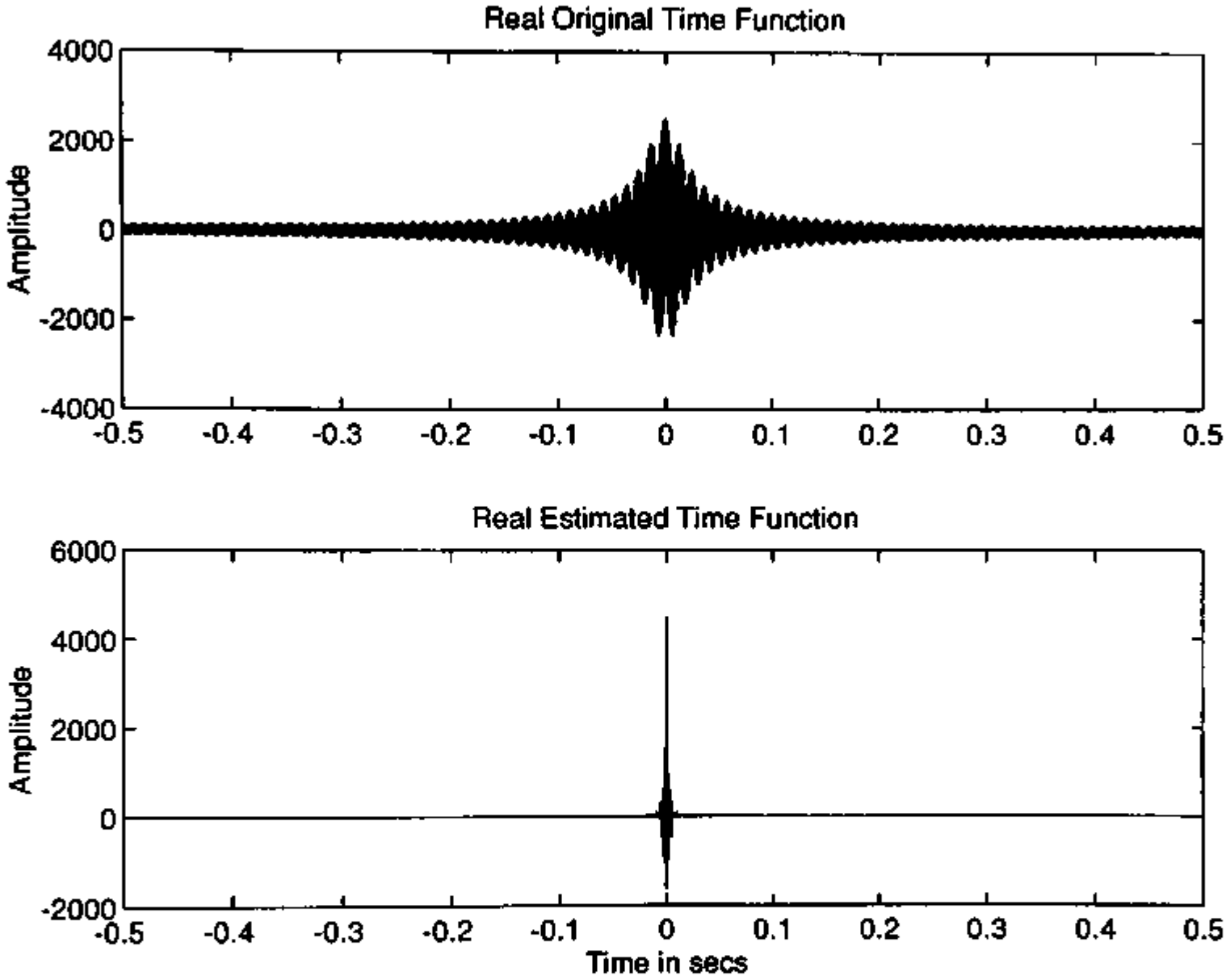

Figure B.2 Continued

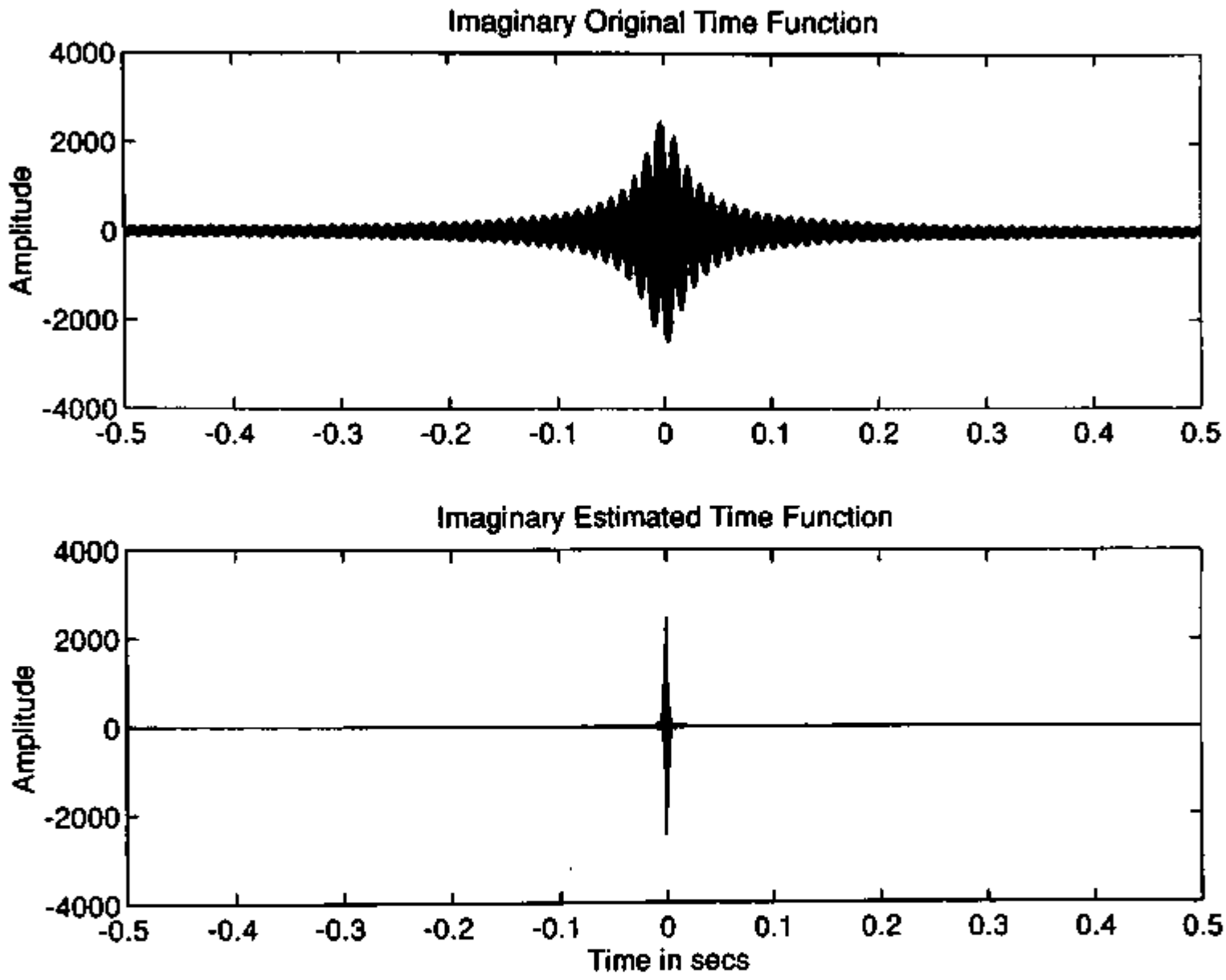

Figure B.2 Continued

CASE B.3

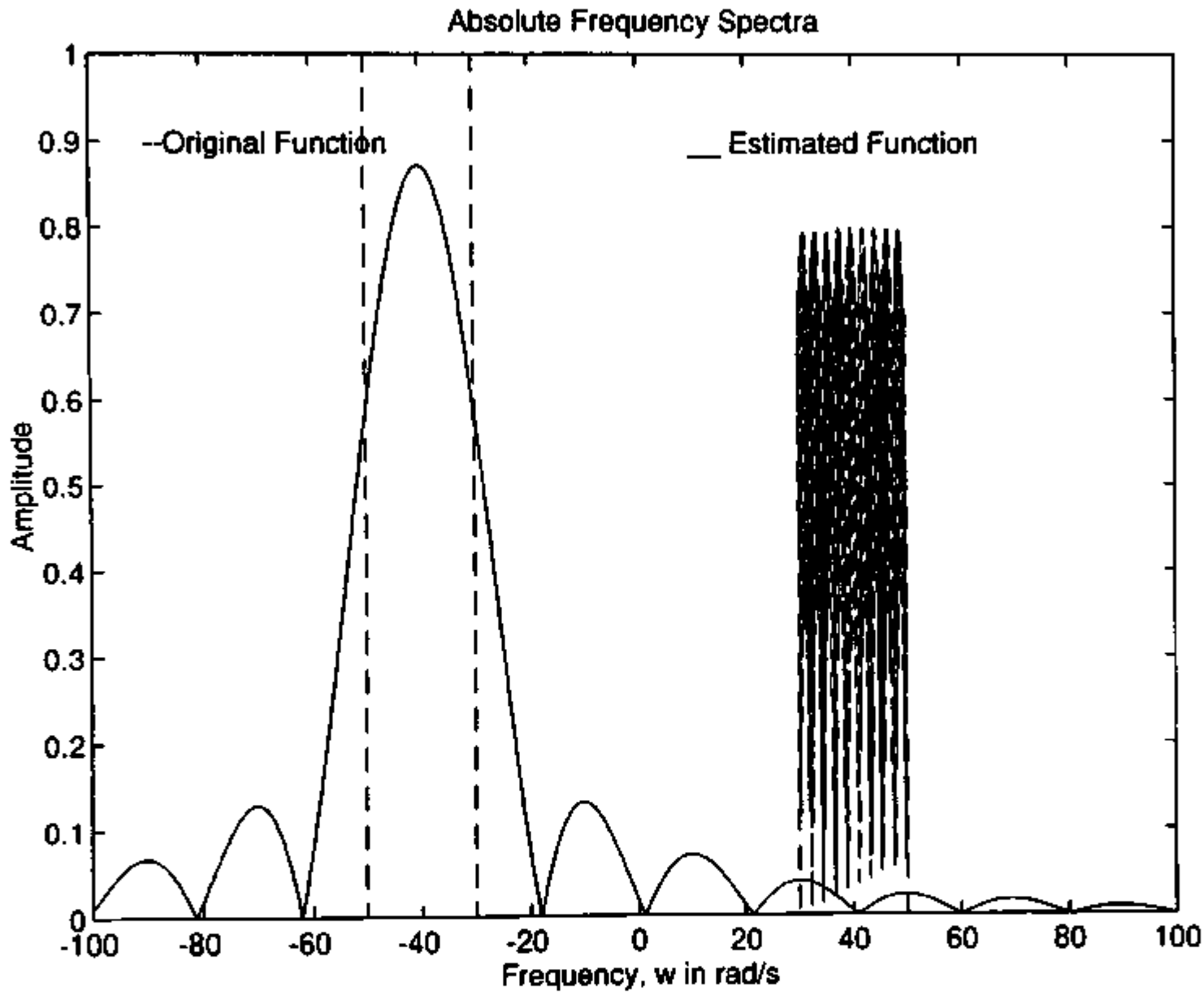

Figure B.3 Results of Case III of Target Density function estimation

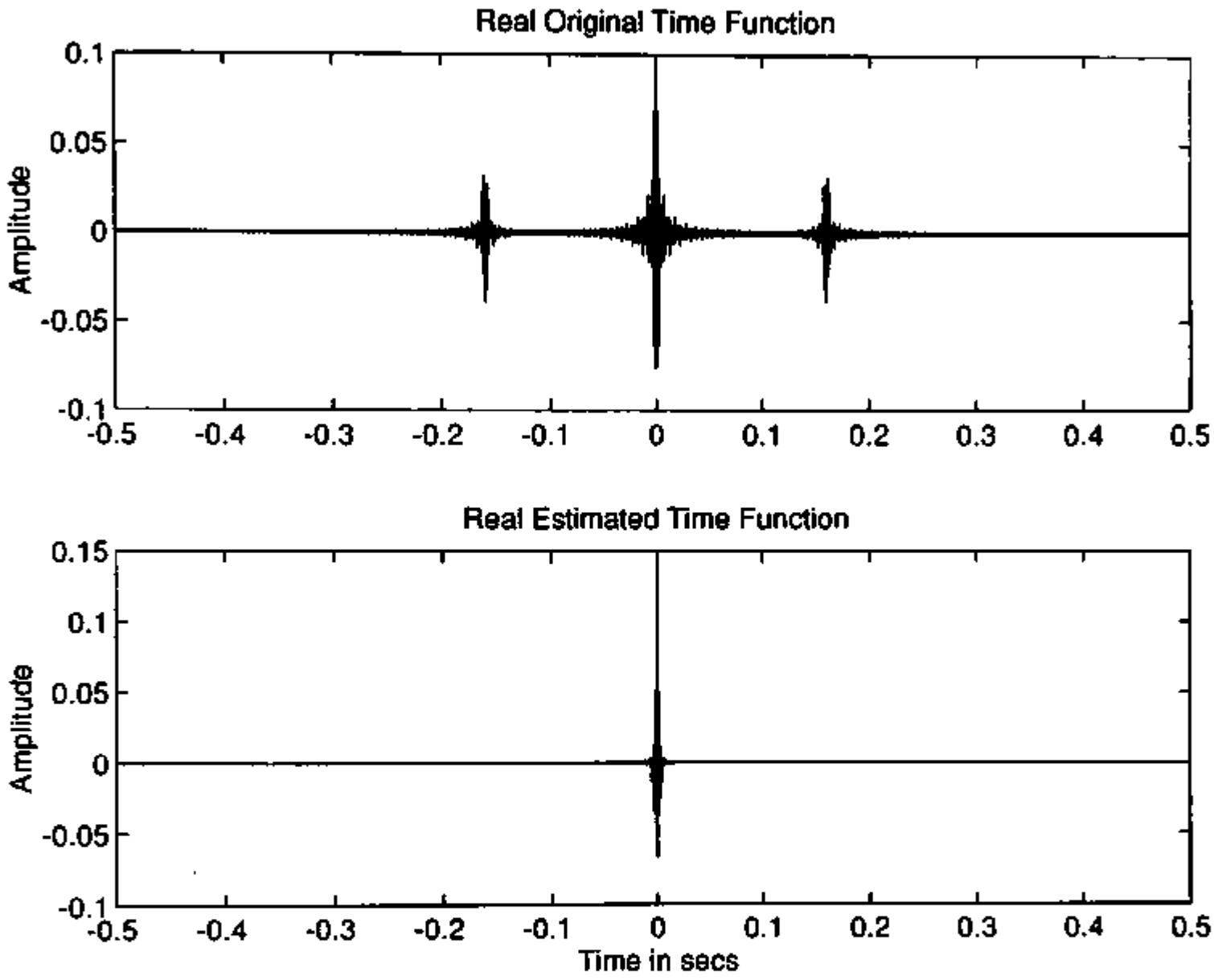

Figure B.3 Continued

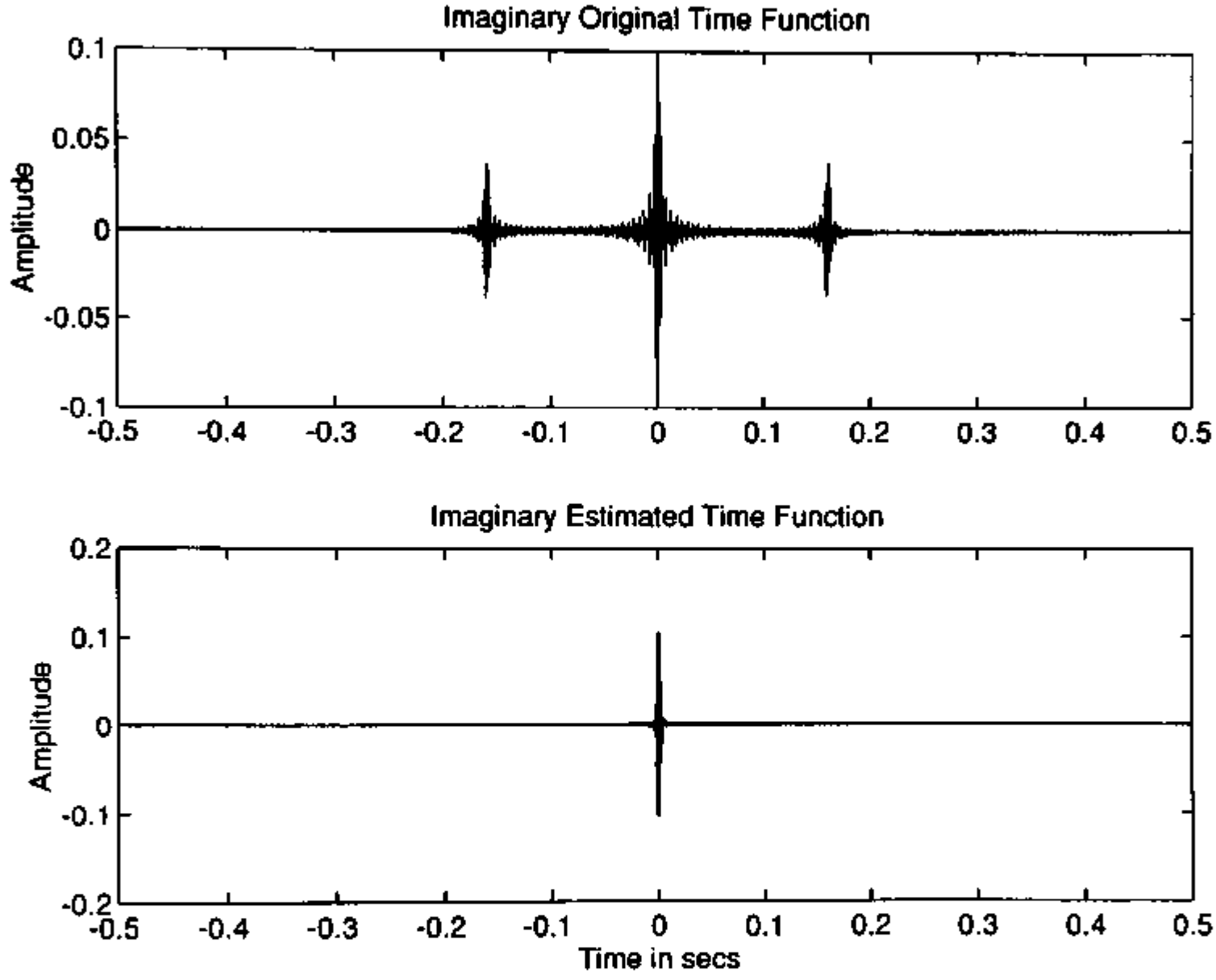

Figure B.3 Continued